Bioactive Materials 34 (2024) 17–36

Contents lists available at ScienceDirect

Bioactive Materials

journal homepage: www.keaipublishing.com/en/journals/bioactive-materials

Transcriptome analysis reveals therapeutic potential of NAMPT in protecting against abdominal aortic aneurysm in human and mouse

Yu Ouyang [a,f,1], Yimei Hong [a,b,1], Cong Mai [a,b,1], Hangzhen Yang [a,g,1], Zicong Wu [c,d], Xiaoyan Gao [b], Weiyue Zeng [b], Xiaohui Deng [c,d], Baojuan Liu [a], Yuelin Zhang [a], Qingling Fu [c,d], Xiaojia Huang [e,***], Juli Liu [e,**], Xin Li [a,b,*]

[a] Department of Emergency Medicine, Guangdong Provincial People's Hospital (Guangdong Academy of Medical Sciences), Southern Medical University, Guangdong, 510006, China
[b] School of Medicine, South China University of Technology, Guangdong, 510006, China
[c] Otorhinolaryngology Hospital, The First Affiliated Hospital, Sun Yat-sen University, 58 Zhongshan Road II, Guangzhou, 510006, China
[d] Extracellular Vesicle Research and Clinical Translational Center, The First Affiliated Hospital, Sun Yat-sen University, Guangdong, 510006, China
[e] Medical Research Institute, Guangdong Provincial People's Hospital (Guangdong Academy of Medical Sciences), Southern Medical University, Guangzhou, 510080, China
[f] Department of Emergency Medicine, The Key Laboratory of Advanced Interdisciplinary Studies , The First Affiliated Hospital of Guangzhou Medical University, Guangzhou, Guangdong 510120, China
[g] Global Health Research Center, Guangdong Provincial People's Hospital (Guangdong Academy of Medical Sciences), Southern Medical University, Guangzhou, 510080, China

ARTICLE INFO

Keywords:
Abdominal aorta
Vascular smooth muscle cells
Senescence
Oxidative phosphorylation
Electron transport chain

ABSTRACT

Abdominal Aortic Aneurysm (AAA) is a life-threatening vascular disease characterized by the weakening and ballooning of the abdominal aorta, which has no effective therapeutic approaches due to unclear molecular mechanisms. Using single-cell RNA sequencing, we analyzed the molecular profile of individual cells within control and AAA abdominal aortas. We found cellular heterogeneity, with increased plasmacytoid dendritic cells and reduced endothelial cells and vascular smooth muscle cells (VSMCs) in AAA. Up-regulated genes in AAA were associated with muscle tissue development and apoptosis. Genes controlling VSMCs aberrant switch from contractile to synthetic phenotype were significantly enriched in AAA. Additionally, VSMCs in AAA exhibited cell senescence and impaired oxidative phosphorylation. Similar observations were made in a mouse model of AAA induced by Angiotensin II, further affirming the relevance of our findings to human AAA. The concurrence of gene expression changes between human and mouse highlighted the impairment of oxidative phosphorylation as a potential target for intervention. Nicotinamide phosphoribosyltransferase (NAMPT, also named VISFATIN) signaling emerged as a signature event in AAA. NAMPT was significantly downregulated in AAA. NAMPT-extracellular vesicles (EVs) derived from mesenchymal stem cells restored NAMPT levels, and offered protection against AAA. Furthermore, NAMPT-EVs not only repressed injuries, such as cell senescence and DNA damage, but also rescued impairments of oxidative phosphorylation in both mouse and human AAA models, suggesting NAMPT supplementation as a potential therapeutic approach for AAA treatment. These findings shed light on the cellular heterogeneity and injuries in AAA, and offered promising therapeutic intervention for AAA treatment.

Peer review under responsibility of KeAi Communications Co., Ltd.
* Corresponding author. Department of Emergency Medicine, Guangdong Provincial People's Hospital (Guangdong Academy of Medical Sciences), Southern Medical University, Guangdong, 510006, China.
** Corresponding author.
*** Corresponding author.
E-mail addresses: huangxiaojia@gdph.org.cn (X. Huang), liujuli@gdph.org.cn (J. Liu), sylixin@scut.edu.cn (X. Li).
[1] The authors contributed equally.

https://doi.org/10.1016/j.bioactmat.2023.11.020
Received 20 August 2023; Received in revised form 7 November 2023; Accepted 28 November 2023
Available online 14 December 2023

1. Introduction

Abdominal aortic aneurysm (AAA) is a condition characterized by the abnormal dilation or bulging of the abdominal aorta. AAA can weaken the arterial wall, increasing the risk of rupture. A ruptured AAA is a medical emergency and can lead to severe internal bleeding, which is often fatal. It is a life-threatening cardiovascular disorder with an approximate 65–85% mortality rate upon rupture [1]. Despite recent advances in surgical intervention techniques and pharmacological therapy, including the use of β-blockers and angiotensin-converting enzyme inhibitors, there is currently no effective treatment that can delay or reverse aneurysm expansion due to unclear underlying mechanisms [2]. Understanding the molecular mechanisms underlying AAA development is crucial for identifying potential therapeutic targets.

Studies showed that cell heterogeneity plays a role in the AAA pathogenesis. Single-cell RNA sequencing (scRNA-seq) provides an opportunity for a comprehensive and unbiased characterization of the molecular profile and heterogeneity of large numbers of individual cells in healthy or AAA aortas [3]. Cell heterogeneity refers to the presence of different cell populations within the aortic wall. For example, vascular smooth muscle cells (VSMCs) are the predominant cell type in the aortic wall and play a crucial role in maintaining vascular integrity and contractility. Our findings demonstrated that AAA induced aberrant switch from a contractile to a synthetic phenotype and cellular senescence in VSMCs [4–6]. This aberrant phenotypic switch is associated with decreased contractility, reduced production of extracellular matrix components, and increased secretion of matrix-degrading enzymes, contributing to the weakening of the aortic wall and the increasing risk of rupture. Therefore, targeting VSMCs is a promising approach to inhibit AAA formation. However, the existence of undiscovered cell types warrants further exploration, urging the continued use of scRNA-seq in deciphering AAA cell heterogeneity.

Aberrant switch from a contractile to a synthetic phenotype and the senescence in VSMCs play critical role in AAA pathogenesis [4–6]. It has been reported that a reduction in Sirtuin 1 (SIRT1) accelerates VSMCs senescence and increases inflammatory cell recruitment for vascular inflammation, leading to formation of an AAA [7]. There is accumulating evidence, including that from our previous studies, that a reduced level of SIRT1, a nicotinamide adenine dinucleotide (NAD^+)-dependent deacetylase, plays a critical role in mediating VSMC senescence in AAA [8,9]. NAD^+, a key coenzyme of hydrogen ion transfer in redox reaction, regulates a variety of physiological activities including aging of cells [10]. NAD^+ positively regulates SIRT1 activity and the NAD^+/SIRT1 pathway represses cellular senescence [11,12]. It has been documented that activation of intracellular NAD^+ level and enhanced SIRT1 activity ameliorated VSMCs senescence induced by angiotensin II (Ang II) [13]. Nicotinamide phosphoribosyltransferase (NAMPT, also named VISFATIN), a rate-limiting enzyme in NAD^+ biosynthesis [14], has been reported to be involved in maintaining many physiological cellular functions via regulation of NAD^+ production [15,16]. Evidence showed that NAMPT expression is disrupted in various diseases and pathophysiological conditions including aging and cardiovascular diseases [17]. NAMPT is expressed in human VSMCs but its activity gradually declines with VSMCs senescence [18]. Our previous study showed that activating NAMPT in VSMCs could inhibit senescence in AAA formation [19], but this remain to be further investigated and the mechanism is unclear. NAMPT is reported to be associated with the generation of adenosine triphosphate (ATP), which is also involved in glycolysis and oxidative phosphorylation [20]. ATP, generated from glycolysis and oxidative phosphorylation processes, is crucial for cell survival and inhibiting senescence [21]. Thus, NAMPT's involvement in ATP generation raises questions about its role in AAA via metabolic regulation. And how NAMPT regulates oxidative phosphorylation-coupled ATP synthesis is unclear, which need to be further investigated.

Mesenchymal stem cell (MSC)-based therapy has shown promising benefits for AAA development and progression. Transplantation of MSCs in mice has been reported to significantly attenuate elastase perfusion–induced AAA formation [22]. Studies have shown that MSCs secrete extracellular vesicles (EVs) [23,24]. More predominately, EVs exert their beneficial effects in cardiovascular disease via transfer of proteins, lipids, and genetic material to injured cells [25,26]. Indeed, transplantation of MSC-EVs has been shown to significantly attenuate aortic aneurysm progression via inhibition of inflammation and promotion of extracellular matrix synthesis [27], suggesting a novel alternative therapeutic strategy for AAA treatment. Nonetheless *in vitro* cultured adult MSCs easily undergo senescence, directly impairing the quality of EVs [28,29]. We successfully generated functional MSCs from human induced pluripotent stem cells (hiPSCs). Compared with adult somatic MSCs, iPSC-MSCs exhibited a higher proliferation potential and lower heterogeneity [30,31]. More importantly, iPSC-MSCs exhibit superior therapeutic efficacy and paracrine actions for cardiovascular diseases than adult MSCs [32]. Whether iPSC-MSC-derived EVs (iPSC-MSC-EVs) ameliorate VSMCs senescence and thus attenuate AAA formation has not been determined. There is increasing recognition that preconditioning or genetic manipulation of MSCs can optimize EVs production and enhance their therapeutic efficacy [33,34]. Since NAD^+, mediated by NAMPT, plays a critical role in regulating VSMCs senescence, whether iPSC-MSC-EVs overexpressing NAMPT (NAMPT-EVs) could provide a better therapeutic effect in AAA also need to be evaluated.

This research utilizes transcriptome techniques to uncover the pivotal role of the NAMPT pathway as a defining event, while also delving into the therapeutic possibilities of NAMPT in both human and mouse models of AAA. We unveil the protective effect of NAMPT-EVs against AAA formation across species. NAMPT-EVs emerge as senescence inhibitors, countering the aberrant shift from contractile to synthetic VSMCs phenotype, and restoring oxidative phosphorylation and the respiratory capability. We underscore the potential of enhancing oxidative phosphorylation coupled ATP synthesis as a promising avenue for AAA treatment.

2. Materials and methods

2.1. Human samples

In this study, abdominal aortas were from three healthy donors (Control) and three patients of abdominal aortic aneurysm (AAA). All human samples shared a common age range, which spanned from 30 to 50 years, and all participants were exclusively male. The AAA patients within our study were individuals who had undergone aortic replacement surgeries at our hospital due to aortic rupture resulting from AAA disease. These samples were meticulously archived in the official tissue biobank at Guangdong Provincial People's Hospital, accompanied by the requisite ethical documentation. The "Control donors" refers to individuals who are healthy but lost their lives under various circumstances, such as car accidents. These individuals have graciously contributed samples for this study.

The study was conducted according to the guidelines of the Declaration of Helsinki, and approved by the Ethics Committee of Guangdong Provincial People's Hospital (No.KY-Z-20210219-02). Informed consent was obtained from all subjects involved in the study.

2.2. Generation of hiPSC-derived MSCs with NAMPT overexpression

The human induced pluripotent stem cells (hiPSCs) were generously provided by the Otorhinolaryngology Hospital at The First Affiliated Hospital of Sun Yat-sen University in Guangzhou, Guangdong, China. The hiPSCs were reprogrammed from human urine-derived cells using electroporation with plasmids containing OCT4, SOX2, SV40LT, and KLF4 (pEP4EO2SET2K). These hiPSCs were cultured on Matrigel (BD Biosciences, USA) and maintained in mTeSR1 (Stem Cell Technologies, Canada).

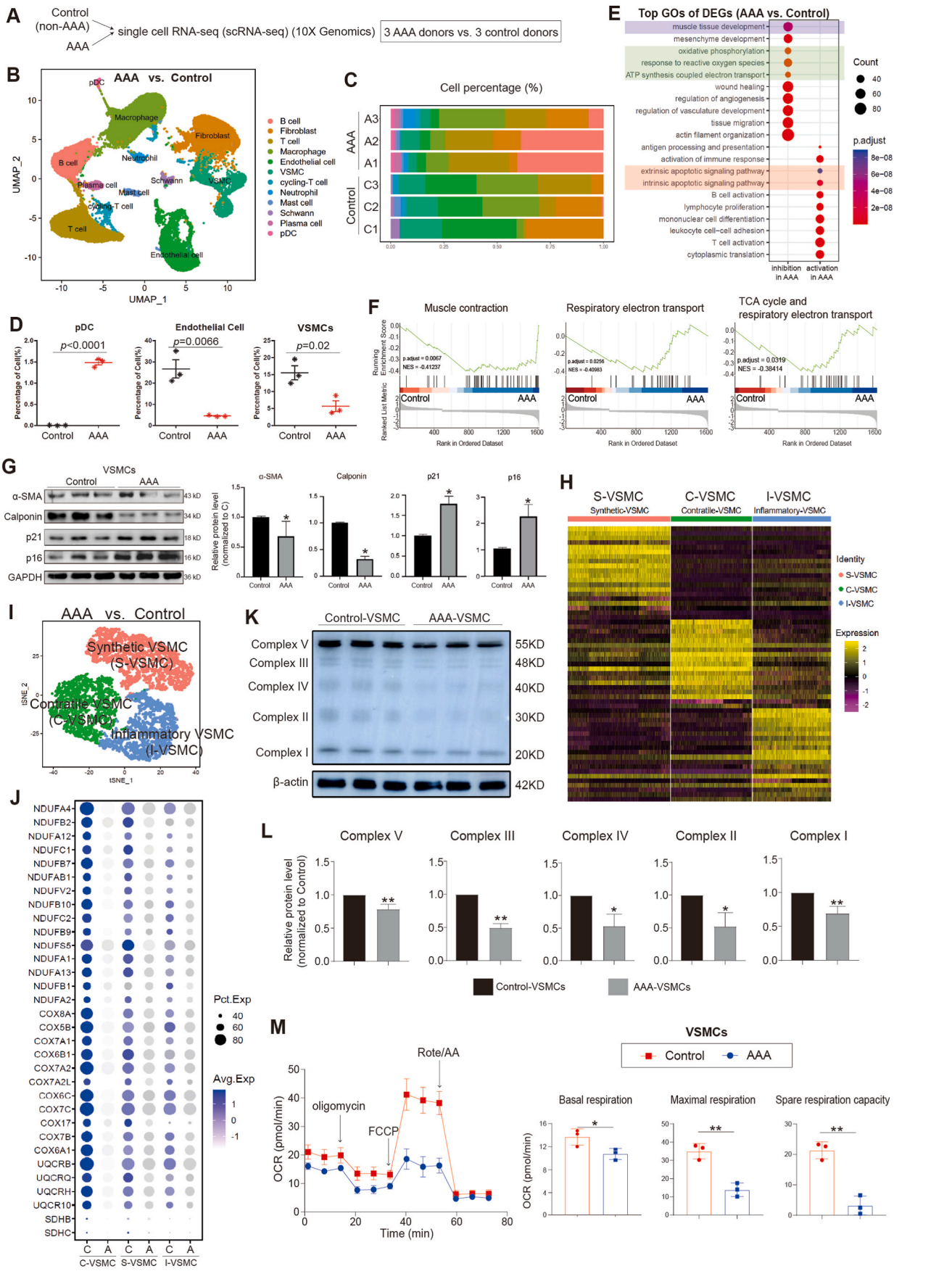

(caption on next page)

Fig. 1. ScRNA-seq reveals cellular injuries and oxidative phosphorylation impairment in abdominal aortic aneurysm (AAA) in human
(A) ScRNA-seq profiling of AAA patient and Control samples. ScRNA-seq was performed on samples from both AAA patients and control subjects. The study included three independent biological replicates for each condition.
(B) Integrated analysis of scRNA-seq data. The visualization of scRNA-seq data was achieved using the uniform manifold approximation and projection (UMAP) technique, revealing the cellular relationships within the dataset.
(C–D) The percentage of different cell types in scRNA-seq. A1, A2 and A3 were three biological replicates of AAA. C1, C2 and C3 were three biological replicates of Control.
(E) Gene Ontology (GO) analysis of differentially expressed genes (DEGs). A, AAA samples.
(F) Gene Set Enrichment Analysis (GSEA) of differentially expressed genes (DEGs) (AAA vs. Control).
(G) Western-blotting showing the expression levels of senescence markers (p21, p16) and VSMCs contractile markers (α-SMA, Calponin). N = 3, p*<0.05.
(H–I) Integrative analysis and re-clustering for VSMCs in scRNA-seq based on gene expression profile. Three main VSMC populations, Inflammatory VSMC (I-VSMC), Contractile VSMC (C-VSMC) and Synthetic VSMC (S-VSMC), were identified.
(J) The expression levels of genes associated with the oxidative phosphorylation in control and AAA. A, AAA. C, Control.
(K) Western-blotting showing the protein expression levels of genes associated with the oxidative phosphorylation and ATP synthesis in VSMCs from control and AAA.
(L) The statistics data from (K). N = 3, p*<0.05; p**<0.01.
(M) Seahorse analysis showing the respiration capacity in VSMCs from control and AAA. N = 3, p*<0.05; p**<0.01. Cell number for one replicate of each group was 1×10^5.

Human iPSC-derived mesenchymal stem cells (MSCs) in this study were prepared as previously described [35]. Briefly, hiPSCs were first dissociated using ethylenediaminetetraacetic acid (EDTA). Subsequently, they were passaged and cultured in six-well culture plates coated with Matrigel (Corning, NY, USA), utilizing mTeSR1 medium (STEMCELL Technologies, Canada). Upon achieving 60% confluency within 2 days, the mTeSR1 medium was replaced with MSC-inducing culture media. This culture medium consisted of minimum essential medium Eagle-α modified (α-MEM; Thermo Fisher Scientific, USA), 10% serum replacement (Stem Cell Technologies, Canada), penicillin/streptomycin, sodium pyruvate, 50 μM L-ascorbate-2-phosphate (Sigma-Aldrich, USA), L-glutamine, and nonessential amino acids. This induction phase lasted for 2 weeks. Following this, the cells were passaged at a 1:2 split ratio as a single-cell suspension using Accutase® (Stem Cell Technologies, Canada) onto gelatin-coated flasks (designated as passage 1 or P1). Subsequently, starting from passage 2 (P2), the cells were passaged using MSC maintenance medium, composed of high-glucose Dulbecco's modified Eagle's medium (Cytiva, USA), 10% fetal bovine serum (FBS; Gibco, USA), basic fibroblast growth factor (Thermo Fisher Scientific, USA), and epidermal growth factor (Thermo Fisher Scientific, USA). After undergoing 3 to 4 passages with this MSC maintenance medium, the cells exhibited a mesenchymal stem cell (MSC)-like phenotype. The induced pluripotent stem cell-derived MSCs (iPSC-MSCs) at passages 10 to 15 were then ready for use in experimental procedures.

The gene encoding human NAMPT (Gene ID: 10135) was PCR-amplified and subsequently inserted into a lentiviral vector. The lentivirus plasmid containing NAMPT was engineered and introduced into HEK 293T cells for lentiviral packaging. Following 48 h of incubation, the supernatant was harvested, concentrated, and tittered. The iPSC-MSCs were seeded in 24-well culture dishes and allowed to incubate for 24 h. Subsequently, they were transfected with the NAMPT lentiviral (at a multiplicity of infection of 100) for a period of 6 h. Two days after the viral infection, the cells were subjected to selection using puromycin (InvivoGen, USA). The efficiency of infection was evaluated by means of fluorescence microscopy and Western blotting analyses.

2.3. Flow cytometry

Surface markers of iPSC-MSCs and NAMPT-iPSC-MSCs were evaluated by flow cytometry. Antibodies including anti-CD90-APC (BioLegend, B322310), anti-CD105-APC (BioLegend, 800507), anti-HLA-DR-APC/Cyanine7 (BioLegend, 307617), anti-CD73-APC (eBioscience, 17-0739-42), anti-CD34-PE (BioLegend, 4341649), anti-CD45-APC (BD, 560973) were used.

2.4. Extracellular vesicles (EVs) derived from iPSC-MSCs

To isolate extracellular vesicles (EVs) from the iPSC-MSCs' conditioned medium, an initial seeding of 1×10^6 iPSC-MSCs was performed in 150 mm cell culture dishes, employing complete culture medium on day 0. Upon reaching a cell density of 70–80% (approximately 1×10^8 cells), the cells were rinsed thrice with 1 × phosphate-buffered saline (PBS), following which the culture medium was substituted with a chemically defined, protein-free medium. Post a 6-h incubation, the medium was aspirated and replaced. After an additional 42 h of incubation, the supernatant enriched with EVs was subjected to centrifugation at 2000 g and 4 °C for 20 min to eliminate cellular debris. iPSC-MSC-EVs were isolated using a scalable anion exchange chromatography procedure [36]. An anion-exchange resin (Q Sepharose Fast Flow; GE Health Care Life Science, Pittsburgh, PA, USA) was packed into an Econo-Pac column (Bio-Rad Laboratories, CD63 Hercules, CA, USA) and equilibrated using Equilibration Buffer. The column was loaded with supernatant, washed with wash buffer to eliminate proteomic contaminants, and then continuously eluted with elution buffer. The fractions with the highest concentration of iPSC-MSC-EVs were pooled in PBS at 4 °C for overnight dialysis. We next utilized Pierce™ Protein Concentrator (Thermo Fisher Scientific, Rockford, IL, USA) to further concentrate the iPSC-MSC-EVs that were then classified according to their morphology and surface marking. The Bradford protein assay and nanoparticle tracking analysis (NanoSight NS300; Malvern, UK) were used to measure the protein and particle concentrations of iPSC-MSC-EVs preparations, respectively.

2.5. Transmission electron microscopy for EVs

The sEV were fixed for 30 min with 2% glutaraldehyde (Sigma, Saint Louis, MO, USA) as described previously [37]. Micrographs of EVs were captured by transmission electron microscope (H7650; HITACHI, Tokyo, Japan).

2.6. Establishment of an AAA model and injection of EVs

All experiments involved animal were approved by Guangdong Provincial People's Hospital for Laboratory Animal Medicine (No. KY2020-105-01). 8 to 10-week-old $ApoE^{-/-}$ male mice on a C57BL/6J background were purchased from GemPharmatech Co. Ltd. and maintained in specific pathogen-free (SPF) conditions. Mice were anesthetized with intraperitoneal pentobarbital sodium (60 mg/kg) and an osmotic minipump (Alzet, Model 2004) implanted subcutaneously into the dorsum of the neck. Ang II (MCE, HY13948) was then infused at a rate of 1000 ng/kg·per min for 28 days. The Control group received saline. Mice with Ang II were randomized to receive the following

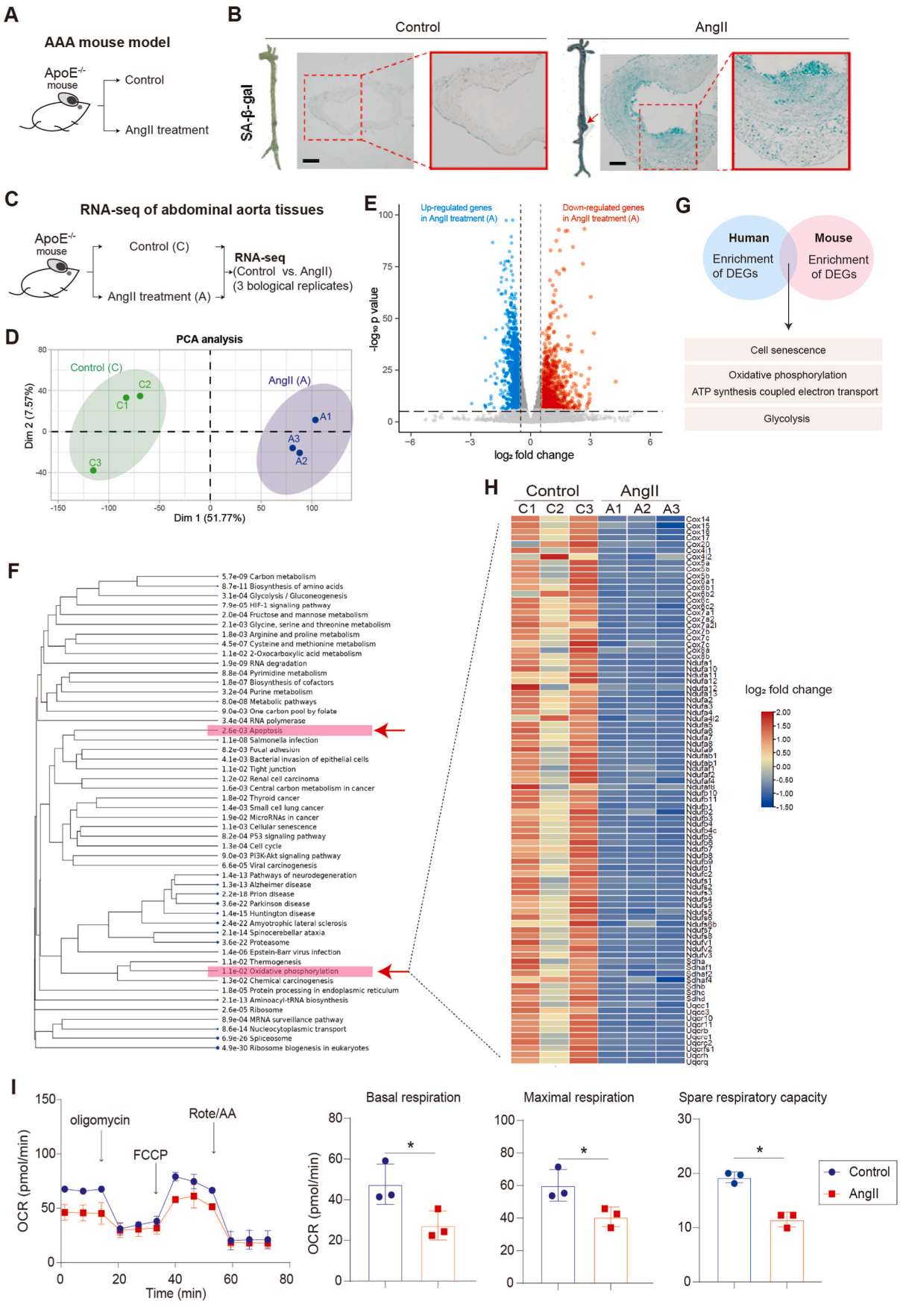

(caption on next page)

Fig. 2. Oxidative phosphorylation are impaired in AAA
(A) The AAA mouse model induced by AngII.
(B) Senescence-Associated β-Galactosidase (SA-beta-gal) staining on abdominal aorta sections of mouse. Scale bar, 200 μm.
(C) RNA-seq analysis of abdominal aortas from Control (C) and AAA (A) mouse. The study included three independent biological replicates for each group.
(D) Principal component analysis (PCA) of RNA-seq data. C1, C2 and C3 were three biological replicates of Control (C). A1, A2 and A3 were three biological replicates of AngII-treatment (A).
(E) Volcano plot showing gene expression patterns between Control (C) and AngII (A).
(F) GO analysis of differentially expressed genes (DEGs) (AngII vs. Control). Red arrows highlighted apoptosis and oxidative phosphorylation.
(G) Comparative analysis of enriched GO terms in human and mouse differentially expressed genes (DEGs). Overlapping analysis of GO terms enriched in DEGs between human and mouse datasets is presented.
(H) Heatmap of differentially expressed genes (DEGs) in oxidative phosphorylation between Control (C) and AngII (A). C1, C2 and C3 were three biological replicates of Control (C). A1, A2 and A3 were three biological replicates of AngII-treatment (A).
(I) Seahorse analysis of oxygen consumption rate (OCR) in Control and AngII-treated mouse VSMCs. N = 3, p*<0.05. Final AngII concentration was 100 nM. OCAR was used to show oxidative phosphorylation process. Cell number for one replicate of each group was 1×10^5.

treatment: (1) PBS (Ang II group), iPSC-MSC-EVs (Control-EVs group), or NAMPT-iPSC-MSC-EVs (NAMPT-EVs group). 2×10^{10} (about 100 μg protein) iPSC-MSC-EVs or NAMPT-iPSC-MSC-EVs were administered intravenously via the tail vein once a week for four weeks. At 28 days, mice were euthanized and placed on a temperature-controlled plate. After removing the hair from the abdomen, an abdominal ultrasound was performed (Visualsonics, Vevo2100). Aneurysm formation was confirmed when the diameter of the suprarenal aorta was ≥ 50% greater than that of mice in the sham group.

2.7. Histological analysis

The entire aorta was fixed with 10% formalin for 24 h at room temperature, embedded in paraffin and sectioned at 5 μm. The embedded aortic tissue was stained with hematoxylin and eosin (IHC World, IW-3100), Masson's stain (Sigma, HT15) or Elastin van Gieson (Sigma, HT25A) using standard protocols. Immunohistochemical staining was carried out with a commercial kit (ORIGENE, PV-6001) and primary antibodies p21 (1:100, 11206, SAB) and p16 (1:400, ab14106, Abcam). Degradation of medial elastic lamina was analyzed by Elastin Van Gieson (EVG) staining and classified as no degradation, mild degradation, severe degradation, or aortic rupture.

2.8. Cell culture and treatment

Human AAA tissue was collected from patients who underwent surgery. Samples of healthy human abdominal aortic tissue were extracted from donors and served as the control group. The procedure was approved by the Guangdong Provincial People's Hospital's research ethics board (No. KY2020-105-01). Written informed consent was obtained from all study subjects. According to our earlier study [8], human vascular smooth cells (VSMCs) used in this study were prepared. Briefly, after removing adventitia and intima and washing with cold PBS, the media was sliced into 1–2 mm^2 pieces and transferred to a 25 cm^2 culture flask, and incubated at 37 °C for 1 h. Once the tissue adhered to the culture flask, medial tissue was cultured with Dulbecco's modified Eagle medium (DMEM; Gibco) supplemented with 15% fetal bovine serum (FBS; Gibco) and 100 μg/mL penicillin and streptomycin (P/S, Thermo Fisher Scientific). Medium was typically refreshed every 3–5 days. VSMCs were evident in the medial tissue after 1–2 weeks. Tissue was subsequently discarded and the cells routinely collected and passaged. In this study, all VSMCs from passage generations 2–4 were used. VSMCs seeded in 6-well plates were then divided into four groups: Control group, Ang II group, Ang II + iPSC-MSC-EVs group and Ang II + NAMPT-iPSC-MSC-EVs group. Except for the control group, all groups were treated with Ang II (100 nM) and EVs (20 μg) for 48 h. In some experiments, in addition to Ang II and EVs treatment, VSMCs were co-cultured with FK866 (2 nM, HY-50876, MCE) and EX527 (1 μM, 49843-98-3, Apollo Scientific).

2.9. EV labelling and uptake by VSMCs

EVs was labeled by PKH67 Green Fluorescent Cell Linker Kit (Sigma, MINI67). 100 μl EV diluted in PBS was added to 200 μl Diluent C. In parallel, 4 μl PKH67 dye was mixed with the above solution and incubated for 4 min. Then 400 μl 0.5% BSA was added and the labeled sEV washed at 100,000g for 1h. Finally, the labeled EVs were diluted in 500 μl DMEM and used for uptake experiments.

2.10. SA-β gal assay

Cellular senescence of VSMCs was examined using a SA-β-gal assay kit (C0602, Beyotime, Shanghai, China). Briefly, VSMCs with different interventions were cultured in 6-well plates. After washing with PBS three times, VSMCs were fixed for 15 min and then stained with SA-β-gal solution overnight at 37 °C without CO_2. Finally, VSMCs with positive SA-β-gal staining, shown in blue color, were randomly imaged under a microscope. Six fields were randomly captured and counted. The ratio of positive VSMCs to the total number of VSMCs was used to evaluate the proportion of senescent VSMCs.

2.11. Western blotting

Total protein of VSMCs and AAA tissues was extracted using RIPA (CST, 9806) and the concentration determined using a bicinchoninic acid (BCA) assay kit (Thermo, 231227). A total of 20 μg protein was resolved by 12% Tris-glycine gel electrophoresis and then transferred to a PVDF membrane. After blocking with 5% skim milk in TBST, PVDF membranes were incubated overnight at 4 °C with the following antibodies: anti-p16 (1:1000, ab51243, Abcam), anti-p21 (1:1000, ab109199, Abcam), anti-NAMPT (1:1000, ab236874, Abcam), anti-γ-H2AX (1:1000, ab81299, Abcam), anti-Calponin (1:2500, ab46794, Abcam), anti-α-SMA(1:1000, AF1032, Affinity) and anti-GAPDH (1:5000, 60004-1-Ig, proteintech). The PVDF membranes were washed three times with TBST and incubated with secondary antibodies (1:2000, 111-035-003, 115-035-003, Jackson) for 1h at room temperature, and then exposed in a dark room. Western blot quantitative detection in three independent experiments was performed using ImageJ software (National Institutes of Health, Bethesda, MD, USA).

2.12. Immunofluorescence staining

Immunofluorescence staining was performed as described previously [38,39]. Briefly, VSMCs were seeded in a 24-well plate with glass coverslips and subjected to different treatments. Next, VSMCs were fixed with 4% paraformaldehyde for 15 min and permeabilized for 30 min with 0.1% Triton X-100 in PBS. After washing with PBS three times, cells were blocked with 10% BSA and incubated overnight at 4 °C with Ki67 antibody (1:1000, 9449T, CST), γ-H2AX antibody (1:500, ab81299, Abcam), α-SMA antibody (1:500, ab5694, Abcam) and calponin antibody (1:500, ab5694, Abcam). Subsequently, VSMCs were washed and

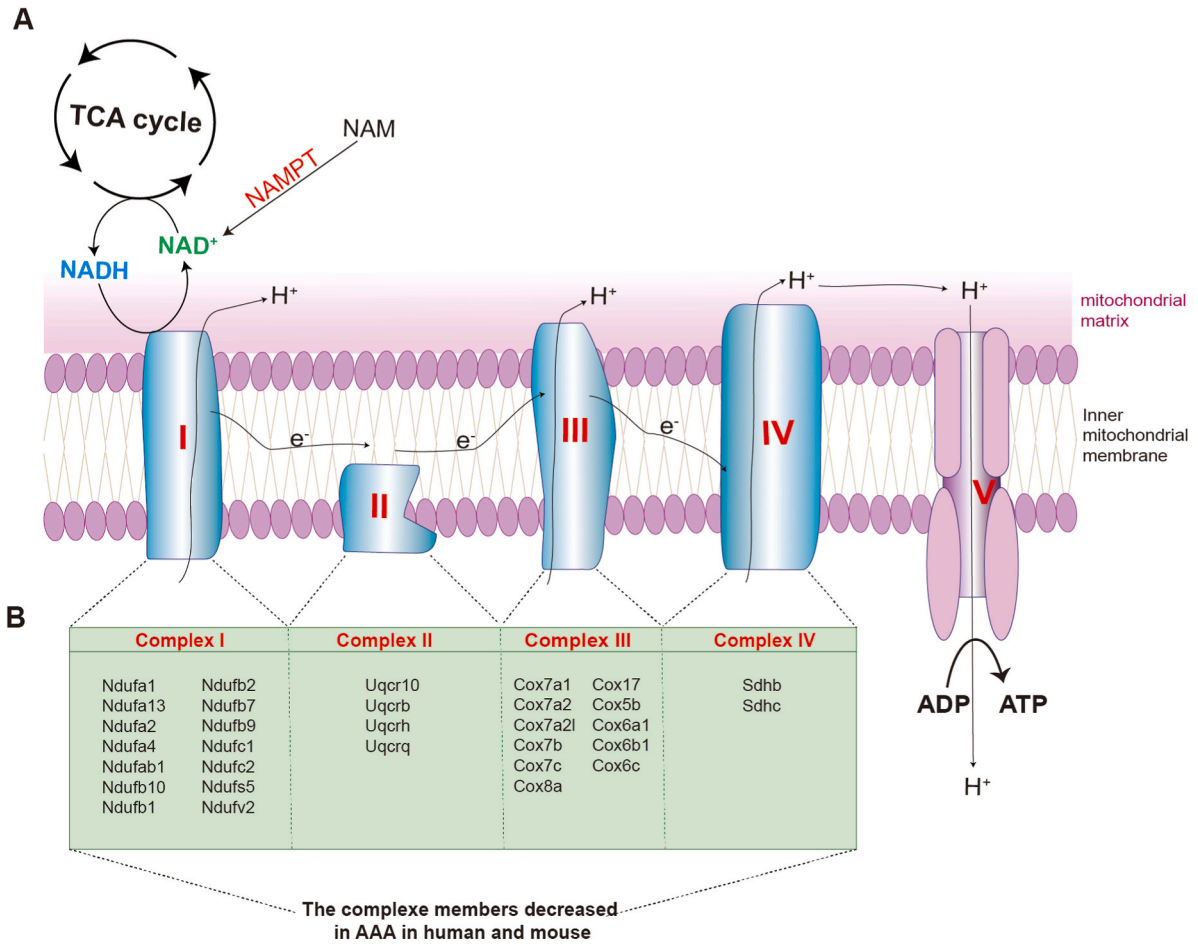

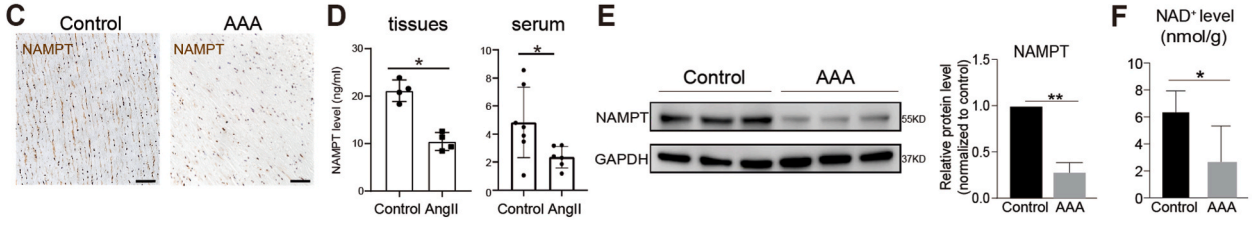

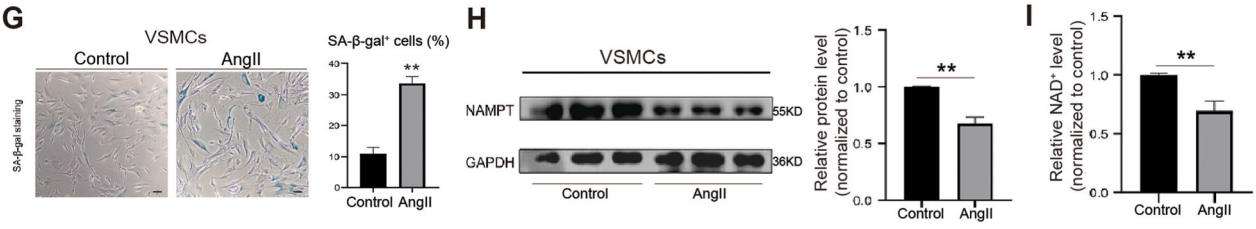

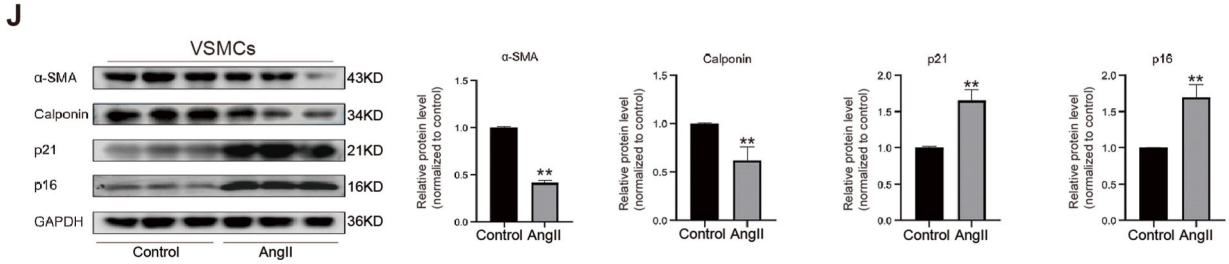

(caption on next page)

Fig. 3. NAMPT is significantly down-regulated in AAA
(A) The relationship of NAMPT, NADH, NAD^+, TCA cycle and oxidative phosphorylation/ATP synthesis. TCA, tricarboxylic acid. e^-, electron. H^+, proton. I, electron transport chain complex (ETC) I. II, ETC complex II. III, ETC complex III. IV, electron transport chain complex IV. NAD^+, Nicotinamide adenine dinucleotide.
(B) The list of genes controlling oxidative phosphorylation/ATP synthesis, which were significantly downregulated in AAA in both human and mouse in this study.
(C) NAMPT staining on human abdominal aortic tissue sections. Scale bar, 200 μm.
(D) ELISA showing the expression levels of NAMPT in human serum and abdominal aortic tissues. For tissue, N = 4, p*<0.01. For serum, N = 4, p*<0.01.
(E) Western-blotting showing the expression levels of NAMPT in human abdominal aortic tissues. N = 3, p**<0.01.
(F) NAD^+ expression level analysis in human VSMCs from control and AAA. N = 3, p*<0.05.
(G) SA-beta-gal staining on human VSMCs isolated from human abdominal aorta. N = 3, p**<0.01. Scale bar, 100 μm
(H) Western-blotting showing the expression levels of NAMPT in human VSMCs with or without AngII treatment. N = 3, p**<0.01.
(I) NAD^+ levels analysis in human VSMCs with or without AngII treatment. N = 3, p**<0.01.
(J) Western-blotting showing the expression levels of markers associated with senescence (p21, p16) and VSMCs contractile (α-SMA, Calponin) in human VSMCs with or without AngII treatment. N = 3, p**<0.01.

incubated with the fluorescent-labeled secondary antibodies (1:500, ab150116, ab150080, Abcam) for 1 h at room temperature in the dark. Finally, glass coverslips were mounted with 4′,6-diamidino-2-phenylindole (DAPI; Vector Laboratories, Inc.) to stain the nucleus. Six view fields from each coverslip were randomly captured with a fluorescent microscope.

2.13. Single-cell RNA-sequencing

2.13.1. Processing of single-cell RNA-seq data

For the human abdominal aortic aneurysm (AAA) samples (3 controls vs 3 AAA patients), the single-cell suspension was loaded on a Single Cell Controller instrument (10 × Genomics, USA) to generate gel beads in emulsions (GEMs). Single-cell RNA-seq libraries were constructed by the Chromium Single Cell 3′ Library & Gel Bead Kit (10 × Genomics, USA) according to the manufacturer's instructions, then sequenced on an Illumina Novaseq 6000. The raw sequenced data was processed using Cell Ranger software (10 × Genomics, USA, version 3.0.2). The reads were aligned to the reference genome hg19 using the STAR aligner, gene expression analysis was performed, including filtering, barcode counting, UMI counting, and finally producing a matrix of gene counts versus cells using the cell count pipeline provided by Cell Ranger. After mapping, six objects were created and performed quality control using the Seurat package (version 4.1.0) in R.

2.13.2. Quality control

To ensure the reliability and accuracy of the data, cells were further filtered according to the following threshold parameters: Genes expressed in fewer than 10 cells were excluded from further analysis. Single cells that expressed more than 300 genes and had less than 20% mitochondrial gene content have been retained. Only cells that met these quality control criteria were included in the downstream analyses. Normalization was performed according to the package manual.

2.13.3. Sample correction and integration

We use the Functions built into Seurat packages to correct for batching effects and merge data sets. The FindIntegrationAnchors function was used to find a set of anchors between six Seurat objects. These anchors can later be used to integrate the objects using the IntegrateData function [40].

2.13.4. Dimensionality reduction and cluster analysis

To reduce the dimensionality of the normalized gene expression values and visualize the cellular heterogeneity, we performed nonlinear dimensional reduction using the Seurat package [41–43]. First, we identified 2000 highly variable genes for the subsequent principal component analysis (PCA). To select the principal components (PCs) that effectively separate the cells, we performed jack straw analysis with 1000 replicates. Based on this analysis, we chose top20 PCs for the t-SNE and UMAP dimensional reduction. The FindClusters function with a resolution of 0.5 was used to identify a total of 12 distinct cell types.

2.13.5. Identification of differentially expressed genes

To identify genes that are differentially expressed across the identified cell types, we employed the Seurat FindAllMarkers and FindMarkers function. This analysis was performed using the normalized gene expression values. By comparing the gene expression profiles between different cell types, we identified unique cell-type-specific marker genes.

2.13.6. Gene Ontology analysis and Gene Set Enrichment Analysis

To gain insights into the potential functions and crucial pathways associated with the identified genes, we performed Gene Ontology (GO) analysis and Gene Set Enrichment Analysis (GSEA) using the ClusterProfiler package (clusterProfiler 4.0). This analysis allowed us to annotate and categorize genes based on their molecular functions, biological processes, and cellular components. Significantly enriched GO terms were determined using the Benjamini-Hochberg adjusted P value threshold of <0.05, significantly enriched GSEA terms were determined using the P value threshold of <0.05 and show the normalized enrichment score (NES), indicating statistical significance.

2.13.7. Cell-cell communication analysis

To investigate cell-cell interactions between different cell types within the samples of Control and AAA, we utilized the CellChat package (version 1.1.2) to analyze and visualize the signaling pathways involved in cell-cell communication.

The "netAnalysis_signalingRole_heatmap" function was employed to display all the different signaling networks between Control and AAA group, and the "netVisual_aggregate" function was employed to display interested signaling networks. Ligand-receptor pairs such as Nampt were specifically examined, providing insights into the potential molecular interactions and communication between cells involved in Nampt pathways.

2.13.8. Cell type Annotation of vascular smooth muscle cells

All 12 cell types are annotated with at least three recognized signatures. Particularly, the classification of subpopulations of VSMCs was mainly based on some published references. The contractile-VSMCs are specifically expressed some famous contractile genes such as MYH11, ACTA2, CNN1, TAGLN, MYLK, MYL9 while the synthetic-VSMCs are associated with the synthesis of ECM genes such as MYH10, COL3A1, COL1A2, COL15A1, FN1, COL8A1 [44–46]. However, unlike macrophage-like-VSMCs previous reported, the inflammatory-VSMCs are highly expressed some inflammatory genes such as complement genes C7, CC chemokine ligand CCL8, CCL19 and CCL21, as well as chemokine CXCL12. What's more, their GO analysis consequences exhibit the functions corresponding to their signatures. The contractile-VSMCs DEGs were significantly enriched in smooth muscle contraction pathway, while the synthetic-VSMCs DEGs were mainly enriched in collagen synthesis and extracellular matrix remodeling pathways [47], and the inflammatory-VSMCs DEGs were involved in some inflammation-related signaling pathways.

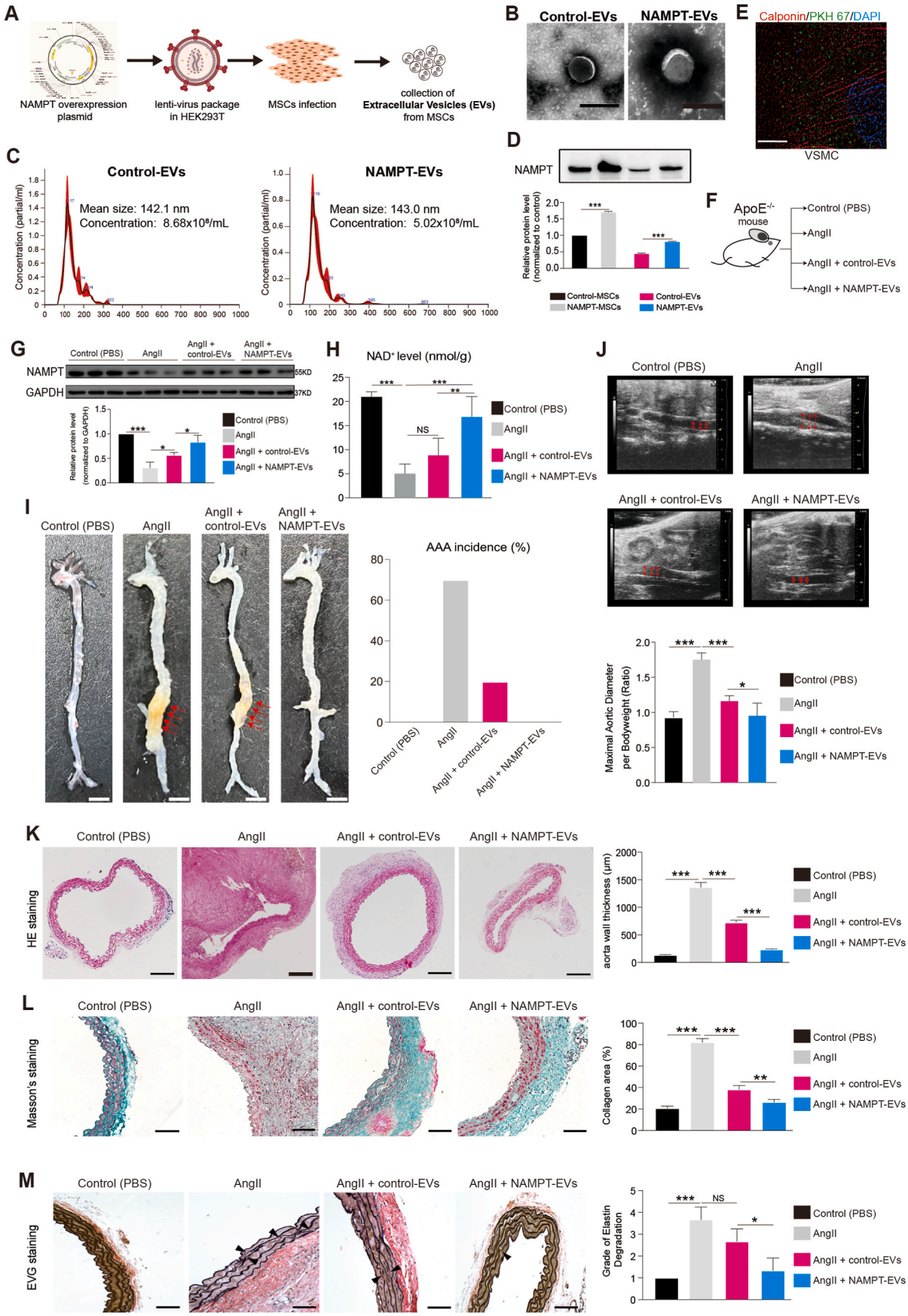

(caption on next page)

Fig. 4. NAMPT extracellular vesicles (NAMPT-EVs) protect against AAA formation in mouse
(A) The scheme of generating NAMPT extracellular vesicles (NAMPT-EVs).
(B–C) Identification of NAMPT-EVs and control-EVs. Scale bar, 200 μm.
(D) Western-blotting analysis of NAMPT in hPSC-MSCs and EVs. N = 3, p***<0.001.
(E) Immunostaining showing expression of EVs marker (PKH67) and VSMCs marker (Calponin). Scale bar, 10 μm.
(F) Evaluation of the therapeutical effect of NAMPT-EVs on AAA mouse model.
(G) Western-blotting analysis of NAMPT in mouse abdominal aorta tissues. N = 3, p*<0.05; p***<0.001.
(H) NAD^+ expression levels analysis in mouse aorta tissues. N = 10, p**<0.01; p***<0.001.
(I) The snapshot images of mouse aortas (left). Scale bar, 5 mm. Red arrows showed the phenotype of abdominal aortic aneurysm. The percentage of AAA incidence was quantified. N = 10.
(J) Ultrasound evaluation of maximal aortic diameter of mouse abdominal aortas. Red arrows showed the maximal aortic diameter. Control group (N = 10), AngII group (N = 6), AngII + control-EVs group (N = 8), AngII + NAMPT-EVs group (N = 10), p*<0.05; p***<0.001.
(K) HE staining of mouse abdominal aorta sections. N = 3, p***<0.001. HE, hematoxylin and eosin. Scale bar, 200 μm.
(L–M) Masson staining (L) and EVG staining (M) of mouse abdominal aorta sections. N = 3, p*<0.05; p**<0.01; p***<0.001. NS, no significance. Masson, Masson's trichrome. EVG, elastin van gieson. Scale bar, 100 μm.

2.13.9. Statistical analysis

Statistical analysis of cell type percentages was conducted using GraphPad Prism 6.0 software. Unpaired Student's *t*-test was used for comparisons between two groups. A p-value of less than 0.05 ($P < 0.05$) is considered to be significant. For the Violin plot showing gene expression differences between Control and AAA groups, statistical analysis was conducted using Wilcox test and $P < 0.05$ are considered significant.

2.14. Bulk RNA-seq

For the bulk RNA-sequencing of mouse aortic samples, vascular smooth muscle cells and Zebrafish model, raw data were generated from BGISEQ platform and reads were filtered and then clean reads were mapped to the reference genome of the corresponding species: Mus musculus reference genome mm39 (GCF_000001635.27_GRCm39) and Zebrafish reference genome danRer11 (GCF_000002035.6_GRCz11), using HISAT software. Then preprocessed reads were mapped to genes with Bowtie2. Bioconductor RNA-sequencing workflow was followed to detect the different expression genes (DEGs) using the DESeq2 statistical package. Gene Ontology and Gene Set Enrichment Analysis was used to identify cellular biologic functions using the ClusterProfiler package. The different expression genes were drawing by EnhancedVolcano package, and the TBtools software and Morpheus interactive tools (Broad Institute) for the heatmap drawing.

2.15. Determination of NAD^+ expression levels

The level of NAD^+ levels in mouse serum, human aortic tissue and cells were determined using a NAD(H) assay kit (BC0315, Solarbio, Beijing, China) according to the manufacturer's instructions.

2.16. Oxygen consumption rate measurements

Human VSMCs (1×10^5 cells) or mouse VSMCs (1×10^5 cells) were seeded in the XF96 cell culture plate (103794-100, Agilent, USA) and placed in a cell culture incubator at 37 °C, 5% CO_2 overnight. The culture medium was replaced with XF Base Medium (pH 7.4) supplemented with 1.0 M Glucose Solution, 100 mM Pyruvate Solution, and 200 mM Glutamine Solution (103793-100, Agilent, USA) after stimulation; it was then incubated in a CO2- free cell incubator at 37 °C for 60 min. OCR was measured using the Seahorse XF cell mito stress test kit (103015-100, Agilent, USA), according to the manufacturer's instructions. Oligomycin (1.5 μM), FCCP (2.0 μM), and Rot/AA (1.0 μM) were added to each well; then, the plate was transferred to a SeaHorseXF96 analyzer (Seahorse XF, Agilent, USA) for analysis.

2.17. Statistical analysis

All values are expressed as mean ± standard deviation (SD). Prism 9.0 software (GraphPad Software for Windows, San Diego, CA, USA) was used to conduct statistical analyses. The unpaired student's t-test is employed to assess mean differences between two groups, whereas one way ANOVA is utilized to examine mean differences among three or more groups. Statistical significance was defined as $p < 0.05$.

3. Results

3.1. ScRNA-seq reveals cell injuries and oxidative phosphorylation impairment in patients with AAA

In this study, we utilized single-cell RNA sequencing (scRNA-seq) to gain a comprehensive and unbiased understanding of the molecular profile and heterogeneity of individual cells from abdominal aortas of control (non-AAA) and AAA patients (Fig. 1A). We identified distinct cell heterogeneity patterns based on gene expression profiles (Fig. 1B–C, Supplemental Figs. 1A–B). Our comparative analysis revealed significant differences in cell type percentages between AAA and Control groups. The percentage of plasmacytoid dendritic cells was notably higher in AAA, while the percentages of endothelial cells and vascular smooth muscle cells (VSMCs) were significantly reduced in AAA compared to the Control group (Fig. 1D, Supplemental Figs. 2A–B). These findings suggested potential involvement of these cell types in the pathogenesis of AAA, although they remain to be further investigated. Global gene expression patterns were also found to differ between AAA and Control samples (Supplemental Fig. 2C). Gene Ontology (GO) analysis highlighted the differentially expressed genes (DEGs) associated with muscle tissue development and apoptotic signaling pathways in AAA (Fig. 1E). Genes controlling phenotypic changes and transitioning from a muscle contractile to a synthetic phenotype, which play important roles in AAA pathogenesis [4–6], exhibited significant enrichment and differential expression between Control and AAA (Fig. 1F). Experimental validation further supported these observations, as the expression level of the muscle contractile marker (α-SMA) was significantly lower in AAA compared to Control (Fig. 1G, Supplemental Fig. 1C), accompanied by increased cell senescence in AAA aortas (Fig. 1G, Supplemental Fig. 1D). We also analyzed gene expression profiling of other cell types (Supplemental Figs. 3A–E). Our findings unveiled a substantial enrichment of collagen re-organization events within these cell populations in the context of abdominal aortic aneurysm (AAA) (Supplemental Figs. 3A–E). This underscores the prominence of collagen and extracellular matrix (ECM) disruption as a leading event in AAA pathogenesis. The ECM, chiefly composed of collagen and elastin, constitutes a pivotal structural element of the aortic wall, and AAA formation ensues from perturbations in proteolytic balance, encompassing ECM matrix remodeling and progressive arterial wall weakening. Our data strongly advocate for the potential therapeutic value in regulating collagen and ECM disruption. Furthermore, our investigation revealed the activation of interferon signaling pathways in macrophages (Supplemental Fig. 3A), fibroblasts (Supplemental

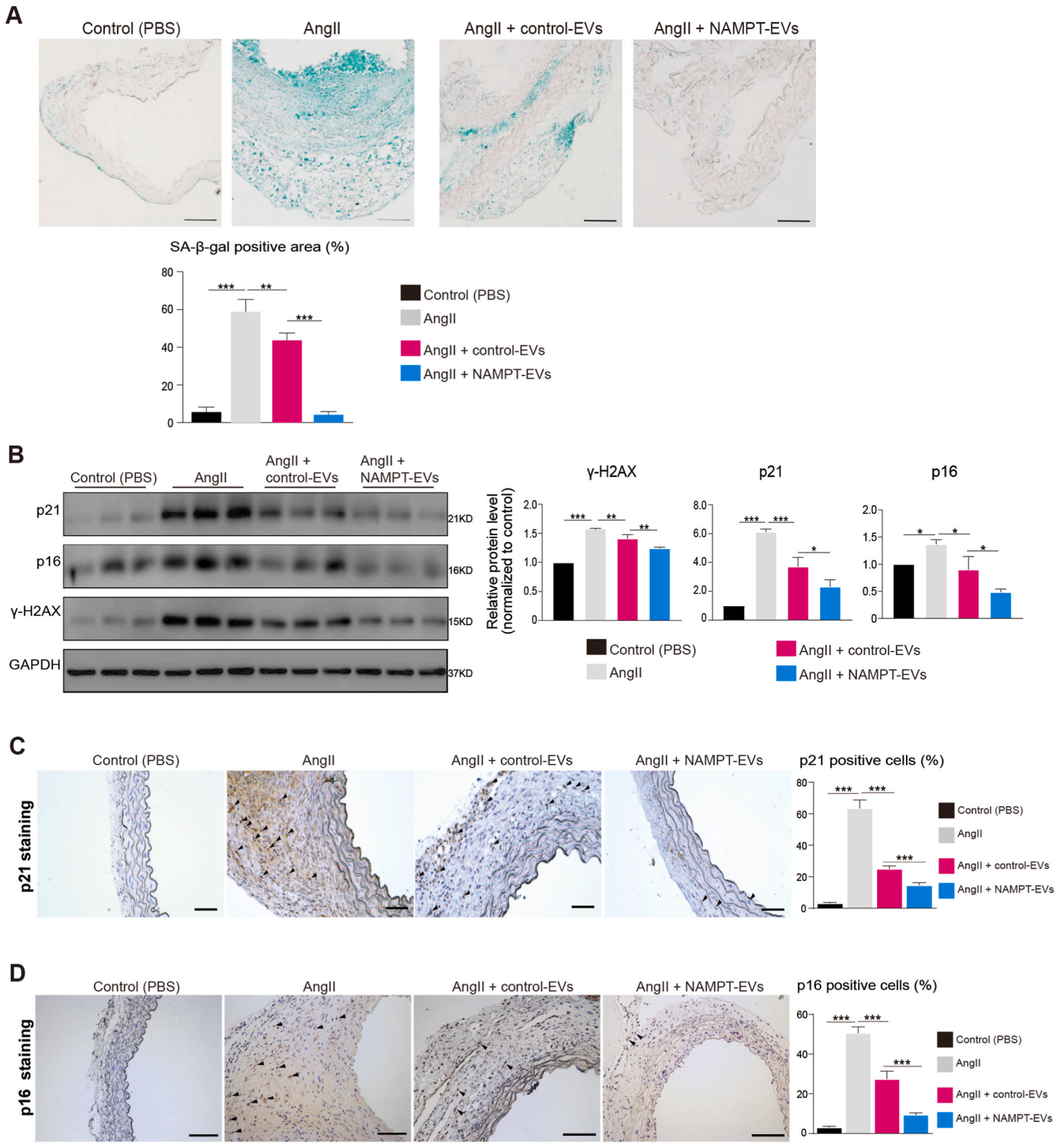

Fig. 5. NAMPT-EVs protect against cellular senescence in mouse AAA

(A) SA-beta-gal staining on mouse abdominal aorta sections. N = 3, p**<0.01; p***<0.001. Scale bar, 5 mm.

(B) Western-blotting showing the expression levels of markers associated with senescence (p21, p16) and DNA damage (γ-H2AX) in mouse abdominal aortas. N = 3, p**<0.01; p***<0.001.

(C–D) p21 (C) and p16 (D) staining of mouse abdominal aorta sections. N = 3, p***<0.001. Scale bar, 500 μm.

Fig. 3B), B cells (Supplemental Fig. 3D), and pDCs (Supplemental Fig. 3E) in AAA. This underscores the significance of interferon signaling in AAA development. Additionally, we observed the enrichment of P53 signaling and cellular senescence events in specific cell types within AAA, notably B cells (Supplemental Fig. 3D), macrophages (Supplemental Fig. 3A), and pDCs (Supplemental Fig. 3E), suggesting that certain cell populations in AAA may undergo cellular death or damage. In terms of metabolic phenotypes, our data indicated the significant repression of genes in citric acid (TCA) cycle and respiratory electron transport chain in macrophages in AAA (Supplemental Fig. 3A),

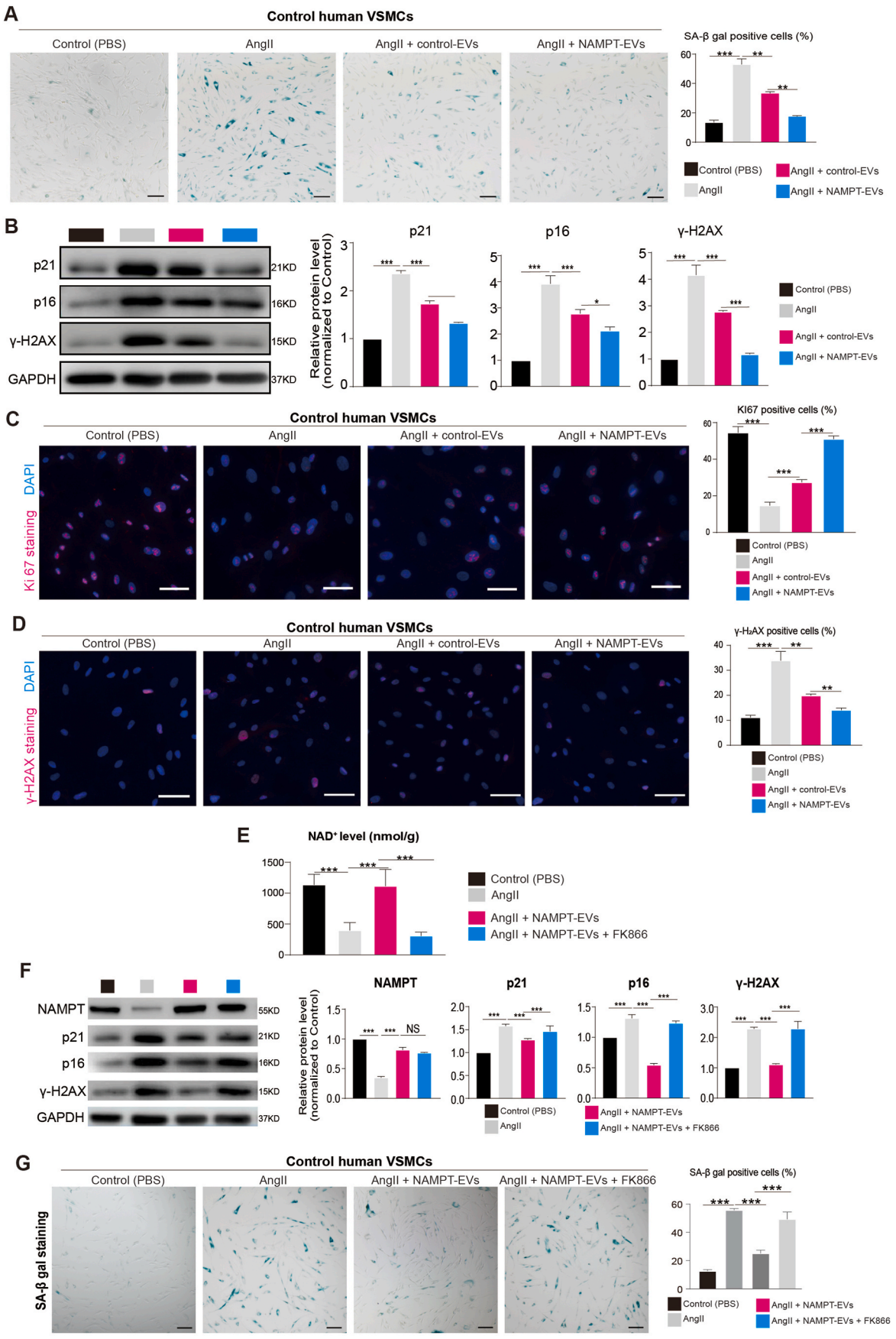

(caption on next page)

Fig. 6. NAMPT-EVs protect against cellular senescence and DNA damage in human AAA model
(A) SA-beta-gal staining on VSMCs isolated from control human abdominal aorta. N = 3, p**<0.01; p***<0.001. Scale bar, 300 μm.
(B) Western-blotting showing the expression levels of markers associated with senescence (p21, p16) and DNA damage (γ-H2AX). N = 3, p*<0.05; p***<0.001.
(C–D) Immunostaining of KI67 (C) and γ-H2AX (D) in VSMCs isolated from control human abdominal aorta. N = 3, p**<0.01; p***<0.001. Scale bar, 300 μm.
(E) NAD^+ expression level analysis in human VSMCs isolated from control abdominal aorta. FK866 is a NAMPT inhibitor. The final concentration of FK886 is 2 nM. N = 3, p**<0.01; p***<0.001. Scale bar, 300 μm.
(F) Western-blotting showing the expression levels of NAMPT and markers associated with senescence (p21, p16) and DNA damage (γ-H2AX). FK866 is a NAMPT inhibitor. The final concentration of FK886 is 2 nM. N = 3, p***<0.001.
(G) SA-beta-gal staining on VSMCs isolated from control human abdominal aorta. N = 3, p***<0.001. FK886, an inhibitor of NAMPT. The final concentration of FK886 is 2 nM. Scale bar, 300 μm.

mirroring the metabolic phenotype observed in vascular smooth muscle cells (VSMCs) in our study, which had not been reported. These findings collectively highlight the diverse roles that different cell types play in the pathogenesis of AAA, warranting further investigation.

Another crucial observation from scRNA-seq was the down-regulation of genes involved in oxidative phosphorylation and ATP synthesis coupled with electron transport in AAA (Fig. 1E and F). We indeed discovered that the genes controlling oxidative phosphorylation and ATP synthesis were significantly down-regulated in AAA compared to control (Supplemental Figs. 4A–B). This indicated an inhibition of oxidative phosphorylation and ATP synthesis in AAA. To further study it, we specifically investigated vascular smooth muscle cells (VSMCs) (Fig. 1H–I, Supplemental Figs. 4C–D), as they are predominant in the aortic wall and play a crucial role in maintaining vascular integrity and contractility [4–6]. Our analysis revealed significant down-regulation of these genes at both RNA level (Fig. 1J) and protein level (Fig. 1K-L) in VSMCs from AAA samples, leading to impaired oxidative phosphorylation and respiration in these cells (Fig. 1M).

Overall, our findings not only revealed unknown distinct cell heterogeneity patterns, but also shed light on the cellular injuries and impaired oxidative phosphorylation observed in patients with AAA. These insights provided a valuable foundation for further research into the mechanisms underlying AAA development and potential therapeutic targets for this disease.

3.2. Oxidative phosphorylation is impaired in AAA in mouse

To account for potential variations, such as ages, genders, and differences in genetic backgrounds in different human samples, and to gain more insight into the pathogenesis of AAA, we established a mouse model of AAA induced by Angiotensin II (AngII) (Fig. 2A), since the infusion of Ang II into hypercholesterolemic $ApoE^{-/-}$ mice has gained popularity as an experimental model for the study of AAA and has successfully replicated several clinical features of human AAA, such as elastin degradation, macrophage infiltration, thrombus formation, and re-endothelialization [48–53]. This model ensured a uniform genetic background and provided more evidence to elucidate the underlying mechanisms of AAA development (Fig. 2A). In our investigation, we observed that AngII administration induced the formation of AAA in mice and led to abdominal aortic cell senescence *in vivo* (Fig. 2B). To explore the gene expression changes associated with AAA, we conducted bulk RNA-seq analysis on both control and AAA mice abdominal aortas (Fig. 2C). The results revealed numerous differentially expressed genes between the AAA and control groups (Fig. 2D–E). Consistent with our observations in human samples (Fig. 1), we found a significant inhibition of oxidative phosphorylation in AAA in mouse (Fig. 2F), accompanied with cell apoptosis (Fig. 2F). This phenocopied the impairment observed in human AAA samples (Fig. 1). To further investigate the similarities between the human and mouse AAA, we overlapped the differentially expressed genes from the scRNA-seq data from human and the bulk RNA-seq data from mice. The overlapping genes were found to be associated with cellular senescence, oxidative phosphorylation, and ATP synthesis coupled with electron transport (Fig. 2G). Furthermore, in line with the results observed in human AAA samples (Fig. 1J-M), the genes controlling oxidative phosphorylation (Fig. 2H) in the AngII-induced AAA aortas were significantly down-regulated compared to those in control mouse aortas. Consequently, this led to a repression of oxidative phosphorylation and respiration (Fig. 2I) in mouse VSMCs treated with AngII.

In summary, our findings provided compelling evidence that oxidative phosphorylation and ATP synthesis is impaired in AAA in both human and mouse. The overlap between the gene expression changes in AAA between human and mouse suggested that mouse AAA model was, at least in part, suitable to recapitulate key aspects of human AAA pathogenesis. Furthermore, the utilization of both human samples and a mouse model represents a more comprehensive approach to corroborating our findings, which provided evidence that improving oxidative phosphorylation and respiration may be a potential therapeutic intervention for AAA.

3.3. NAMPT is significantly down-regulated in AAA

In order to understand the differential events and underlying molecular mechanisms controlling AAA formation, we initially conducted cell-cell communication and interaction analyses based on differentially expressed genes between control and AAA human samples, which unveiled several potential regulatory events implicated in AAA (Supplemental Figs. 4E–F). Among these events, the Nicotinamide phosphoribosyltransferase (NAMPT, also named VISFATIN) signaling pathway stood out as a signature feature (Supplemental Fig. 4F). NAMPT plays a critical role in the biosynthesis of nicotinamide adenine dinucleotide (NAD^+) (Fig. 3A–B) [54]. The completion of the tricarboxylic acid (TCA) cycle generates ATP and the byproduct NADH that further feed the electron transport chain complex I and complex II, respectively (Fig. 3A–B). Complexes I and II then pass their electrons through the electron transport chain complex to ultimately produce ATP through oxidative phosphorylation (Fig. 3A–B). And our earlier discovery revealed a substantial repression of genes responsible for electron transport complex and oxidative phosphorylation/ATP synthesis (Figs. 1–2, Fig. 3A). Thus, all these evidence led us to hypothesize that NAMPT may be involved in oxidative phosphorylation and ATP synthesis in AAA pathogenesis. Previous study had reported a potential protective effect of NAMPT in thoracic aortic aneurysm (TAA) [55,56]. However, the therapeutic potential of NAMPT supplementation in AAA and the underlying molecular mechanisms require further elucidation. Therefore, we finally directed our focus towards understanding NAMPT's function in AAA. In our investigations, we observed a significant decrease in NAMPT protein expression in VSMCs from AAA patient abdominal aorta tissues (Fig. 3C–E) and serum (Fig. 3D), which consequently led to a reduction in NAD^+ levels in abdominal aorta tissues (Fig. 3F). In the *in vitro* AAA model of human VSMCs induced by AngII, we found that AngII caused senescence in human VSMCs (Fig. 3G–H) and significantly reduced NAMPT protein expression (Fig. 3H), resulting in decreased NAD^+ levels in human VSMCs (Fig. 3I). Additionally, AngII induced senescence and promoted phenotypic changes and the transition from a contractile to a synthetic phenotype in human VSMCs, as evidenced by decreased expression of contractile markers (α-SMA, Calponin) and increased expression of senescence markers (p21, p16) (Fig. 3J). These findings collectively demonstrated that the NAMPT may play a pivotal role in human AAA pathogenesis.

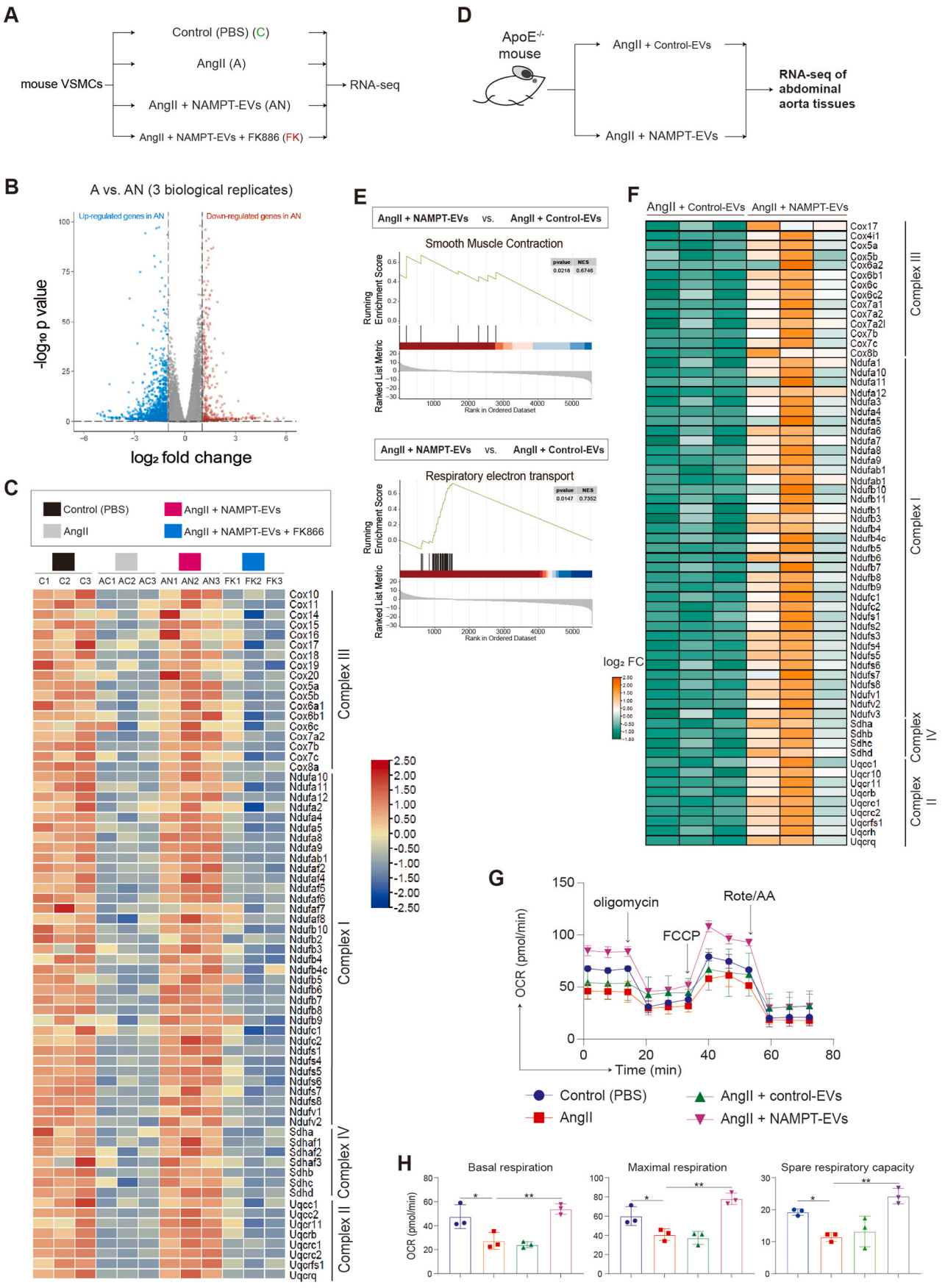

(caption on next page)

Fig. 7. NAMPT-EVs rescue oxidative phosphorylation in protecting against AAA
(A) RNA-seq analysis of mouse VSMCs. Three biological replicates were applied for RNA-seq
(B) Volcano plot showing the differentially expressed genes (DEGs) (A vs. AN). Threshold of $p < 0.05$ and $|\log2 \text{ (fold change)}| > 1$ was used to define DEGs.
(C) Heat map showing the expression levels of genes involved in Respiratory electron transport and ATP synthesis.
(D) RNA-seq of mouse abdominal aorta tissues. Three biological replicates were applied.
(E) GSEA analysis of differentially expressed genes (DEGs) from (D). Smooth muscle contraction and Respiratory electron transport/ATP synthesis events were enriched.
(F) Heat map showing the expression levels of genes involved in Respiratory electron transport and ATP synthesis. FC, fold change.
(G–H) Seahorse analysis of oxygen consumption rate (OCR) in mouse VSMCs. N = 3, p*<0.05. Final AngII concentration was 100 nM. OCAR was used to show oxidative phosphorylation. Cell number for one replicate of each group was 1×10^5.

3.4. NAMPT protects against cellular injuries and AAA formation in mouse

On the other hand, NAMPT can circulate extracellularly in EVs in the bloodstream, specifically in plasma and serum, while simultaneously residing intracellularly within the cytoplasm, mitochondria, and nucleus of the majority of cells [57–59]. On the other hand, establishing a drug delivery system into target cells is crucial for disease therapy. Studies had consistently demonstrated the beneficial effects of mesenchymal stem cells (MSCs)-secreted extracellular vesicles (EVs) in tissue repair [23,24]. Therefore, the EVs may be the promising drug delivery system. Based on this, we sought to study NAMPT function and explore whether EVs containing NAMPT protein could be a promising therapeutic approach for AAA treatment. To investigate this potential therapy, we genetically modified human induced pluripotent stem cells (hiPSCs)--derived MSCs to overexpress NAMPT (Fig. 4A, Supplemental Figs. 5A–C), and we collected the EVs secreted from the iPSC-MSCs (Fig. 4A–C). The NAMPT protein level in the NAMPT-EVs was significantly higher than that in the Control-EVs (Fig. 4D, Supplemental Fig. 5D). Furthermore, we confirmed that these EVs could effectively transport into VSMCs by labeling the EVs marker PKH67 on VSMCs (Fig. 4E).

For *in vivo* evaluation, we administered the EVs (Control-EVs or NAMPT-EVs) into mice with AAA induced by AngII (Fig. 4F, Supplemental Fig. 5E). In the AAA mouse model, AngII treatment led to a decrease in NAMPT protein expression in mouse abdominal aorta tissues, while NAMPT-EVs administration successfully restored NAMPT protein levels (Fig. 4G). AngII treatment also resulted in reduced NAD^+ levels in mouse abdominal aorta tissues, which were reversed by NAMPT-EVs administration (Fig. 4H). Crucially, we observed that mice treated with AngII had a higher incidence of AAA compared to control mice (Fig. 4I–J). However, when NAMPT-EVs were administered, the AAA formation was significantly inhibited (Fig. 4I–J). Histochemistry staining of abdominal aorta sections showed that NAMPT-EVs effectively attenuated AngII-mediated AAA development (Fig. 4K-M). Moreover, NAMPT-EVs mitigated cellular senescence and DNA damage induced by AngII in AAA mouse model (Fig. 5A–D).

In conclusion, our findings highlighted the potential of iPSC-MSC-derived NAMPT-EVs as a promising therapeutical approach for treating AAA in mouse. These EVs, enriched with NAMPT, not only restored NAMPT protein expression and NAD^+ levels but also exhibited a protective effect against AAA development in an *in vivo* model.

3.5. NAMPT protects against injuries in human AAA model

To investigate the potential protective effects of NAMPT in *in vitro* human AAA cells, we conducted experiments using human VSMCs isolated from abdominal aortas of control (non-AAA) donors. We specifically examined the impact of NAMPT-EVs on cellular injuries induced by AngII. Our results revealed that AngII treatment led to cell senescence in human VSMCs, but this senescence could be mitigated by NAMPT-EVs treatment (Fig. 6A). Additionally, NAMPT-EVs treatment effectively reduced the upregulation of markers associated with senescence (p21, p16) and DNA damage (γ-H2AX) induced by AngII (Fig. 6B). Moreover, NAMPT-EVs treatment rescued $KI67^+$ cells (Fig. 6C), which are indicative of cell proliferation. Furthermore, we observed that NAMPT-EVs treatment reduced the presence of $\gamma\text{-H2AX}^+$ (Fig. 6D), which is a marker of DNA damage. To further validate the specificity of NAMPT's effects on human VSMCs, we employed the specific NAMPT inhibitor, FK866 [60] (Fig. 6E). We found that FK866 decreased the upregulation of NAD^+ level induced by NAMPT-EVs in human VSMCs (Fig. 6E). Consequently, the beneficial effects of NAMPT-EVs on human VSMCs could be halted when FK866 was used, reinforcing the role of NAMPT in protecting against cellular injuries, such as cell senescence and DNA damage (Fig. 6F–G).

Collectively, our findings demonstrate that NAMPT plays a crucial protective role in a human AAA VSMCs. NAMPT-EVs effectively mitigate AngII-induced cellular senescence, enhance cell proliferation, and reduce DNA damage, showcasing the potential therapeutic benefits of NAMPT in preserving cellular integrity and counteracting injuries in human VSMCs. This also phenocopied the results from AAA mouse model (Figs. 4–5).

3.6. RNA-seq reveals that NAMPT-EVs rescue oxidative phosphorylation in protecting against AAA

To gain further insights about the underlying mechanism, we performed bulk RNA-seq on mouse VSMCs (Fig. 7A–B, Supplemental Figs. 6A–C). Our analysis revealed that the gene expression patterns between the control group and the NAMPT-EVs-treated group were similar, indicating that NAMPT-EVs had a protective effect on mouse VSMCs (Supplemental Fig. 6D). Conversely, the gene expression patterns between the AngII group and the NAMPT-EVs plus FK886 group displayed analogous trends, underscoring the substantial role of NAMPT in shielding AngII-treated VSMCs (Supplemental Fig. 6D). Enrichment analysis of differentially expressed genes between "AngII + NAMPT-EVs" group with AngII only group showed that NAMPT-EVs not only attenuated the expression levels of collagen genes induced by AngII (Supplemental Fig. 6E), but also rescued expression levels of genes which controlling oxidative phosphorylation and ATP synthesis (Fig. 7C, Supplemental Fig. 6E). We extended our investigation to *in vivo* mouse AAA model by using RNA-seq to determine if the effects of NAMPT were consistent with that in the *in vivo* model (Fig. 7D). Our analysis revealed that genes promoting smooth muscle cell contraction were rescued after NAMPT-EVs treatment (Fig. 7E). Furthermore, we observed a restoration in genes governing oxidative phosphorylation and respiratory coupled ATP synthesis (Fig. 7E–F, Supplemental Fig. 7A), resulting in the reduction of intracellular ROS generation (Supplemental Fig. 7B). Moreover, our investigations revealed that respiratory capacity of mouse VSMCs were inhibited after AngII treatment (Fig. 7G–H). However, administration of NAMPT-EVs efficiently counteracted these inhibitory effects of AngII, resulting in the restoration of respiratory capacity (Fig. 7G–H). These evidences showed that NAMPT could rescue oxidative phosphorylation in protecting against AAA.

Taken together, our findings demonstrated that NAMPT effectively rescued oxidative phosphorylation in the context of AAA. The supplementation of NAMPT hold promise as a potential therapeutic approach for AAA treatment, primarily attributed to its ability to restore ATP synthesis.

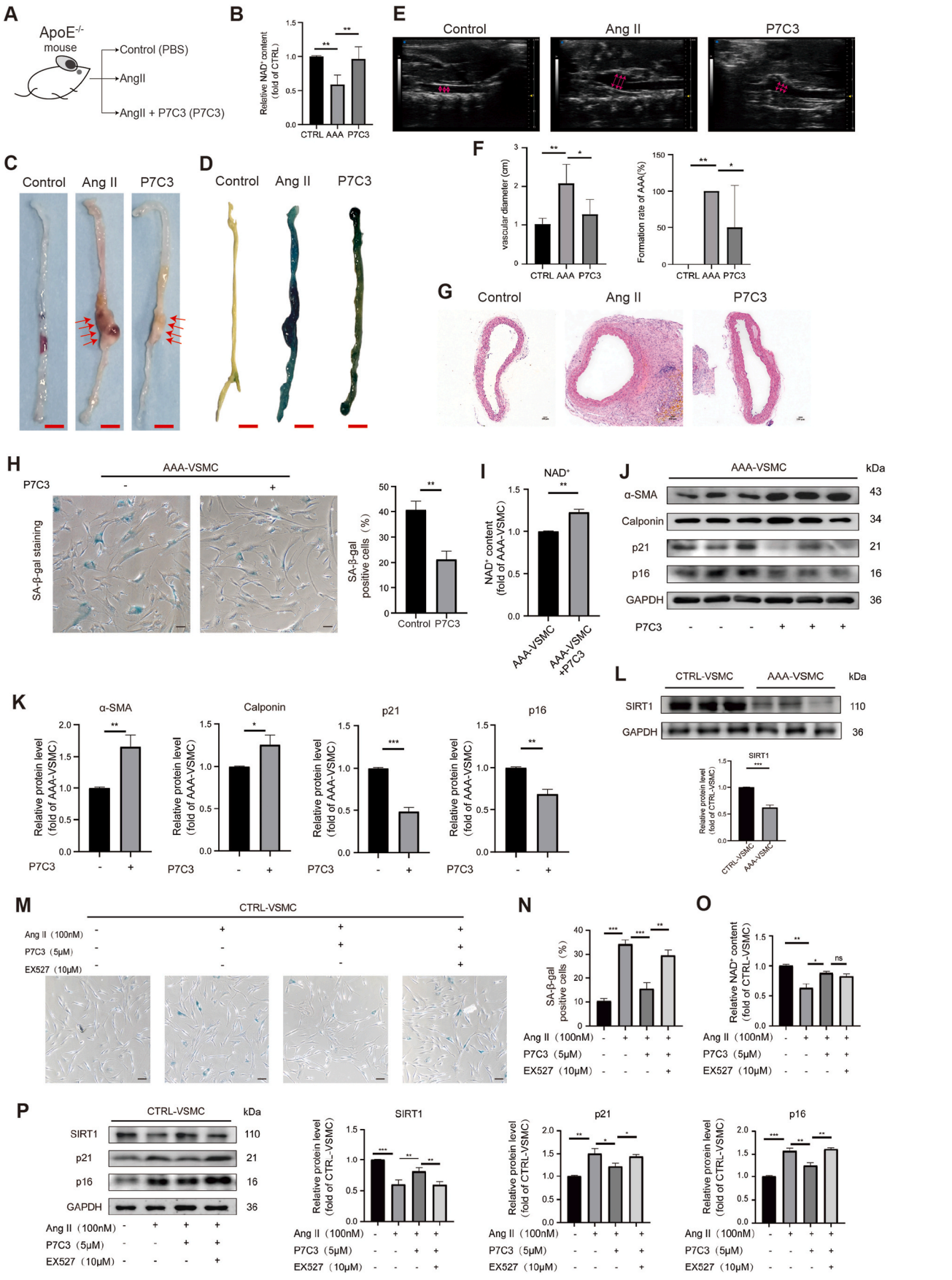

(caption on next page)

Fig. 8. NAMPT activation protects against AAA *in vitro* and *in vivo*
(A) The scheme to study the function of NAMPT activation by its activator P7C3 in AAA pathogenesis. The concentration of P7C3 injected into mouse was 5 μM.
(B) NAD^+ expression level analysis in mouse abdominal aortas. CTRL, control. CTRL, N = 5; AngII, N = 4; P7C3, N = 5; p**<0.01.
(C) The snapshot images of mouse abdominal aortas. Scale bar, 5 mm. Red arrows showed the phenotype of abdominal aortic aneurysm.
(D) The SA-beta-gal staining of mouse abdominal aortas. Scale bar, 5 mm.
(E–F) Ultrasound evaluation of mouse abdominal aortas. Red arrows showed the maximal aortic diameter. CTRL, control (Sham), N = 5; AngII, N = 4; P7C3, N = 5; p*<0.05; p**<0.01. (G) HE staining of mouse abdominal aorta sections. HE, hematoxylin and eosin. Scale bar, 100 μm.
(H) The SA-beta-gal staining of human AAA VSMCs. The concentration of P7C3 treated on cells was 5 μM. N = 3; p**<0.01. Scale bar, 100 μm.
(I) NAD^+ expression level analysis in human AAA VSMCs. The concentration of P7C3 treated on cells was 5 μM. N = 3; p**<0.01. (J–K) Western-blotting showing the expression levels of markers associated with senescence (p21, p16) and VSMCs contractile phenotype. The concentration of P7C3 treated on cells was 5 μM. N = 3; p*<0.05, p**<0.01, p***<0.001.
(L) Western-blotting showing the expression of SIRT1 on human control and AAA VSMCs. N = 3; p***<0.001.
(M–N) The SA-beta-gal staining of human control VSMCs. EX-527, a selective SIRT1 Inhibitor. The concentration of P7C3 treated on cells was 5 μM. The concentration of EX527 treated on cells was 10 μM. N = 3; p**<0.01, p***<0.001. Scale bar, 100 μm.
(O) NAD^+ expression level analysis in human control VSMCs. EX-527, a selective SIRT1 Inhibitor. The concentration of P7C3 treated on cells was 5 μM. The concentration of EX527 treated on cells was 10 μM. N = 3; p*<0.05, p**<0.01.
(P) Western-blotting showing the expression levels of markers associated with senescence (p21, p16) and SIRT1 in human control VSMCs. N = 3; p*<0.05, p**<0.01, p***<0.001.

3.7. NAMPT activation protects against AAA in vivo and in vitro

To gain further insights about NAMPT and the potential therapeutical approaches targeting NAMPT, we evaluated whether the chemical P7C3, a NAMPT agonist, can be used for AAA treatment. We found that in AAA mouse model (Fig. 8A) P7C3 increased NAD^+ level (Fig. 8B). P7C3 mitigated AngII-induced AAA phenotypes *in vivo* (Fig. 8C–G). We also tested P7C3 effect on human VSMCs *in vitro*. We found that P7C3 reduced cellular senescence in AAA-VSMCs (Fig. 8H) and increased NAD^+ level (Fig. 8I). P7C3 increased protein expression levels of VSMCs markers which inhibit the switch from synthetic phenotype to contractile phenotype (Fig. 8J–K). P7C3 also decreased protein expression levels of markers of cellular senescence (Fig. 8J–K). This indicated that NAMPT agonist mitigates AAA development. Furthermore, we found that SIRT1 was repressed in AAA-VSMCs (Fig. 8L). We evaluated whether NAMPT could protect against AAA via SIRT1. Thus, we employed EX527, a SIRT1 inhibitor. We found that EX527 aggravated P7C3-mitigated cellular senescence in AngII-induced AAA model *in vitro* (Fig. 8M − P). This data demonstrated that NAMPT activation protects against AAA *in vivo* and *in vitro*, at least in part, via SIRT1.

4. Discussion

In this study, we utilized transcriptome analysis to reveal the intricate molecular mechanisms underlying abdominal aortic aneurysm (AAA) pathogenesis. By integrating scRNA-seq and bulk RNA-seq analyses in both human and mouse AAA models, we gained valuable insights into cellular heterogeneity, injuries, and impaired oxidative phosphorylation associated with AAA. Our findings not only collectively contribute to a comprehensive understanding of AAA development, but also highlight the potential therapeutic role of NAMPT in mitigating the disease.

One of the contributions of scRNA-seq in this study is the characterization of distinct cell heterogeneity patterns based on gene expression profiles. We firstly identified higher percentage of plasmacytoid dendritic cells (pDCs) in AAA samples compared to controls. Study showed that plasmacytoid dendritic cell activation may be associated with AAA [61], but the study did not find the percentage of pDCs was changed in AAA and the underlying mechanisms in pDCs activation was unclear. Higher percentage of pDCs in AAA, which was newly found in our study, suggests that pDCs may potentially contribute to the progression of AAA, which needs to be further studied. On the other hand, the reduction in percentages of endothelial cells and vascular smooth muscle cells (VSMCs) in AAA samples may indicate their dysfunction or depletion in the AAA aortas, which are similar with our previous findings [4–6]. VSMCs, in particular, are critical for maintaining vascular integrity and contractility, and their reduced abundance in AAA could be a significant factor contributing to the weakening of the aortic wall and aneurysm formation. Our findings emphasize the complex interplay between diverse cell populations in AAA development and warrant further investigations into the roles of these cells, such as pDCs, in disease progression.

The global gene expression patterns revealed through scRNA-seq and enrichment analysis offer valuable insights into the underlying molecular mechanisms involved in AAA development. The up-regulated genes associated with smooth muscle tissue development/contraction and apoptotic signaling in AAA indicate the presence of active remodeling processes and increased cell death in the AAA aortic wall. Of particular interest are the genes controlling the aberrant phenotypic changes in VSMCs, transitioning them from a contractile to a synthetic phenotype. This observation in our study suggests that VSMCs undergo a shift in their characteristics, potentially losing their contractile ability and adopting a more synthetic phenotype associated with matrix remodeling and inflammation, which could contribute to the progression of AAA. The experimental validation supporting the scRNA-seq findings further strengthens the significance of the observed molecular changes in AAA. The reduced expression of the muscle contractile markers in AAA samples and the accompanying increase in cell senescence provide evidence of VSMCs dysfunction and aging in AAA. These changes in VSMCs could lead to compromised aortic wall integrity, making it more susceptible to aneurysm formation and rupture, suggesting that targeting VSMCs will be a potential intervention for AAA treatment.

The connection between NAMPT, NAD+, NADH, the tricarboxylic acid cycle (TCA cycle), oxidative phosphorylation, and ATP synthesis hints at a potential interplay. NAMPT assumes a pivotal function in the production of nicotinamide adenine dinucleotide (NAD+) [54]. The tricarboxylic acid (TCA) cycle's successful completion results in the production of ATP and the byproduct NADH, which subsequently supply electrons to electron transport chain complex I and complex II, respectively. Complexes I and II, in turn, transfer these electrons along the electron transport chain to ultimately generate ATP through oxidative phosphorylation. Our earlier findings indicated a significant suppression of genes responsible for the electron transport complex and oxidative phosphorylation/ATP synthesis. These accumulated pieces of evidence, along with the enrichment of the NAMPT pathway in cell-cell communication as revealed by our scRNA-seq analysis, led us to propose the hypothesis that NAMPT may have a role in oxidative phosphorylation and ATP synthesis during the development of AAA. As a result, we delved into the NAMPT (VISFATIN) signaling pathway and uncovered NAMPT's pivotal role in AAA. Thus, the omics, such as scRNA-seq in this study, provided new helpful information for understanding the molecular mechanisms underlying AAA pathogenesis and development.

NAD^+, a key coenzyme of hydrogen ion transfer in redox reaction,

regulates a variety of physiological activities including aging of cells [10]. Recent study showed that supplementation of Nicotinic acid, a precursor of NAD^+, might protect against AAA formation [53]. The study showed the importance of NAD^+ signaling pathway in repressing AAA formation. Nicotinamide phosphoribosyltransferase (NAMPT) is a rate-limiting enzyme in NAD^+ biosynthesis [14]. In our study, we identified the NAMPT signaling pathway as a signature event in human AAA. NAMPT, a critical player in cellular metabolism and NAD^+ biosynthesis, is downregulated in both human and mouse AAA samples. Our previous study showed that activating NAMPT in VSMCs could inhibit senescence in AAA formation [19], but the mechanism is unclear. How to develop an approach for AAA treatment is also crucial for patients. Mesenchymal stem cell (MSC)-based therapy has shown promising benefits for AAA development and progression due to its low toxicity and immunogenicity [62]. Transplantation of MSCs in mice has been reported to significantly attenuate elastase perfusion–induced AAA formation [22]. In particular, MSC-derived EVs are composed of factors such as cytokines, growth factors, RNA, and miRNAs, which originate from MSCs and thus exert similar effects to those of MSCs. And the therapeutic potential of mesenchymal stem cell-derived EVs is more enhanced than MSCs itself [63]. Many evidences showed that no signs of toxicity on MSC-EVs were observed, and minimal evidence of changes in immune markers were noted [64–67]. Studies have shown that extracellular vesicles (EVs) secreted by MSCs [23,24], exert their beneficial effects in cardiovascular disease via transfer of genetic material to injured cells [25,26]. However, whether EVs containing NAMPT have therapeutic potential is unclear. The use of MSC-derived NAMPT-enriched extracellular vesicles (EVs) in our study as a potential therapeutic approach for AAA treatment in the mouse model adds another layer of significance.

NAMPT is found to circulate both extracellularly in the bloodstream, particularly in plasma and serum, and intracellularly within the cytoplasm, mitochondria, and nucleus of the majority of cells [57–59]. Substantial evidence suggests that extracellular NAMPT is exclusively present in extracellular vesicles (EVs) in both mice and humans [68], and the release of NAMPT in EVs under physiological conditions plays a vital role in cellular function [69,70]. NAMPT has the potential to elevate NAD^+ levels, which can have a positive impact on health and potentially extend lifespan [69]. Notably, NAMPT protein cannot be internalized independently; it relies on the internalization of extracellular vesicles (EVs) containing NAMPT to enter target cells [69]. This observation led us to incorporate NAMPT into EVs derived from MSCs, mimicking physiological conditions in humans, which holds promise for enhanced therapeutic efficacy. This approach in our study also underscores the advantages of using EVs as a delivery system for NAMPT supplementation. Thus, compared to various interventions, such as CTRP13 [56] and Niacin [53]. Our approach is notably more direct and advantageous for several reasons: (1) NAMPT can circulate both within the bloodstream, specifically in plasma and serum, and intracellularly within the cytoplasm, mitochondria, and nucleus of various cell types [57–59]; (2) A wealth of evidence indicates that extracellular NAMPT is exclusively packaged within EVs in both mice and humans [68]; (3) The release of NAMPT within extracellular vesicles under physiological conditions plays a pivotal role in modulating cellular functions [69,70]. By harnessing the capacity to load NAMPT into EVs, we aim to faithfully replicate physiological conditions in humans, thereby offering a more promising avenue for therapy.

Another crucial aspect uncovered in this study is the downregulation of genes involved in oxidative phosphorylation in AAA samples. Oxidative phosphorylation is a critical metabolic process that occurs in the mitochondria, generating adenosine triphosphate (ATP), the primary energy currency of cells. It involves the transfer of electrons through the electron transport chain (ETC) to produce a proton gradient across the mitochondrial inner membrane. This proton gradient drives the synthesis of adenosine triphosphate (ATP) from adenosine diphosphate (ADP) and inorganic phosphate (Pi) through the action of ATP synthase [71]. Mitochondrial damage induces respiratory chain impairment via disrupting oxidative phosphorylation, which leads to reduced ATP synthesis, the molecular unit carrying intracellular energy, and may further increase generation of ROS [21], which was also observed in our study. This indicated that the impairment of oxidative phosphorylation and ATP synthesis may promote AAA progression. Previous studies showed that differential expression of several genes associated with mitochondrial function and oxidative phosphorylation were enriched in AAA [72,73], but whether these genes lead to respiratory inhibition in aortic cells is still unclear. Recent studies revealed some cellular pathways involved in mitochondrial oxidative phosphorylation [74]. The study did not further investigate how oxidative phosphorylation was affected by using experimental methods. P53 was reported to be involved in oxidative phosphorylation in AAA in caloric restriction (CR) model [75]. This study found that abnormal energy metabolism-mediated by P53 contributes to the aggravated AAA formation in mice, indicating the relationship between oxidative phosphorylation-coupled ATP synthesis and AAA development. Their study was not involved in NAMPT function and the oxidative phosphorylation. Here, our study not only found genes governing oxidative phosphorylation were significantly inhibited in AAA, but also further confirmed the impairment of cellular respiratory capacity in VSMCs in AAA. Importantly, we discovered that NAMPT-EVs protected against AAA formation, in which the oxidative phosphorylation and cellular respiratory capacity were rescued. This finding in our study highlights the importance of oxidative phosphorylation and the coupled respiratory capacity in maintaining a healthy aortic wall, which also suggests that improving oxidative phosphorylation by NAMPT will be a potential therapeutic approach for AAA treatment. To corroborate the findings in human samples and to explore potential therapeutic targets for AAA, we established an AngII-induced AAA mouse model. The phenotypic similarities observed between the human and the mouse AAA model strengthen the translational significance of the mouse AAA model, suggesting its reliability in studying AAA pathogenesis. Importantly, the impairment of oxidative phosphorylation observed in the mouse AAA model is consistent with the findings in human samples, further emphasizing the relevance of this process in AAA development. In our study, NAMPT also showed conservative protection against AAA across different species.

5. Conclusion

In conclusion, this study provides a comprehensive and multifaceted analysis of the cellular injuries and impaired oxidative phosphorylation observed in AAA. By combining scRNA-seq data and bulk RNA-seq from human samples, *in vitro* human cell model and an AngII-induced AAA mouse model, we revealed valuable insights into the molecular mechanisms underlying AAA development. The identification of the NAMPT signaling pathway as a signature event in human AAA, along with the evaluation of therapeutic effects of NAMPT-EVs in both human and mouse models, highlights the potential of NAMPT as a therapeutic approach for treating AAA. These findings offer a solid foundation for further translational research and the development of potential therapeutic interventions for this life-threatening condition. However, it is essential to acknowledge that additional studies, including more preclinical, will be necessary to validate the efficacy and safety of NAMPT-based therapies for AAA and to further delineate the detailed mechanisms about oxidative phosphorylation in AAA.

Availability of data and materials

All data have been included in the paper. The datasets used in this study are available from the corresponding author on reasonable request.

Ethics approval and consent to participate

The study was conducted according to the guidelines of the Declaration of Helsinki, and approved by the Ethics Committee of Guangdong Provincial People's Hospital (No.KY-Z-20210219-02). Informed consent was obtained from all subjects involved in the study.

CRediT authorship contribution statement

Yu Ouyang: Data curation, Formal analysis, Investigation, Methodology, Software, Validation, Visualization, Writing – review & editing. **Yimei Hong:** Data curation, Formal analysis, Investigation, Methodology, Project administration. **Cong Mai:** Investigation, Methodology, Project administration, Validation. **Hangzhen Yang:** Data curation, Formal analysis, Investigation, Methodology, Project administration, Validation, Writing – review & editing. **Zicong Wu:** Resources, Software. **Xiaoyan Gao:** Resources, Software. **Weiyue Zeng:** Resources, Software. **Xiaohui Deng:** Resources. **Baojuan Liu:** Resources. **Yuelin Zhang:** Resources. **Qingling Fu:** Resources. **Xiaojia Huang:** Data curation, Formal analysis, Software, Writing – review & editing. **Juli Liu:** Conceptualization, Data curation, Formal analysis, Investigation, Methodology, Resources, Software, Visualization, Writing – original draft, Writing – review & editing. **Xin Li:** Conceptualization, Funding acquisition, Resources, Supervision, Writing – review & editing, Project administration, Visualization.

Declaration of competing interest

The authors declare that they have no competing interests.

Acknowledgement

We thank all fundings. This research was funded by the National Natural Science Grant of China (No. 82072225, 82272246); High-level Hospital Construction Project of Guangdong Provincial People's Hospital (No. DFJHBF202104; No. DFJH201918); Science and Technology Program of Guangzhou, China (No. 202206010044); Guangdong Basic and Applied Basic Research Foundation (2021B1515120062).

Appendix A. Supplementary data

Supplementary data to this article can be found online at https://doi.org/10.1016/j.bioactmat.2023.11.020.

References

[1] N. Sakalihasan, J.B. Michel, A. Katsargyris, H. Kuivaniemi, J.O. Defraigne, A. Nchimi, J.T. Powell, K. Yoshimura, R. Hultgren, Abdominal aortic aneurysms, Nat. Rev. Dis. Prim. 4 (2018) 34.
[2] K.E. Kristensen, C. Torp-Pedersen, G.H. Gislason, M. Egfjord, H.B. Rasmussen, P. R. Hansen, Angiotensin-converting enzyme inhibitors and angiotensin II receptor blockers in patients with abdominal aortic aneurysms: nation-wide cohort study, Arterioscler. Thromb. Vasc. Biol. 35 (2015) 733–740.
[3] G. Zhao, H. Lu, Z. Chang, Y. Zhao, T. Zhu, L. Chang, Y. Guo, M.T. Garcia-Barrio, Y. E. Chen, J. Zhang, Single-cell RNA sequencing reveals the cellular heterogeneity of aneurysmal infrarenal abdominal aorta, Cardiovasc. Res. 117 (2021) 1402–1416.
[4] K. Yang, J. Ren, X. Li, Z. Wang, L. Xue, S. Cui, W. Sang, T. Xu, J. Zhang, J. Yu, et al., Prevention of aortic dissection and aneurysm via an ALDH2-mediated switch in vascular smooth muscle cell phenotype, Eur. Heart J. 41 (2020) 2442–2453.
[5] Y. Zhang, X. Huang, T. Sun, L. Shi, B. Liu, Y. Hong, Q.L. Fu, Y. Zhang, X. Li, MicroRNA-19b-3p dysfunction of mesenchymal stem cell-derived exosomes from patients with abdominal aortic aneurysm impairs therapeutic efficacy, J. Nanobiotechnol. 21 (2023) 135.
[6] X. Huang, H. Zhang, X. Liang, Y. Hong, M. Mao, Q. Han, H. He, W. Tao, G. Jiang, Y. Zhang, X. Li, Adipose-derived mesenchymal stem cells isolated from patients with abdominal aortic aneurysm exhibit senescence phenomena, 2019, Oxid. Med. Cell. Longev. (2019), 1305049.
[7] H.Z. Chen, F. Wang, P. Gao, J.F. Pei, Y. Liu, T.T. Xu, X. Tang, W.Y. Fu, J. Lu, Y. F. Yan, et al., Age-associated Sirtuin 1 reduction in vascular smooth muscle links vascular senescence and inflammation to abdominal aortic aneurysm, Circ. Res. 119 (2016) 1076–1088.
[8] W. Tao, Y. Hong, H. He, Q. Han, M. Mao, B. Hu, H. Zhang, X. Huang, W. You, X. Liang, et al., MicroRNA-199a-5p aggravates angiotensin II-induced vascular smooth muscle cell senescence by targeting Sirtuin-1 in abdominal aortic aneurysm, J. Cell Mol. Med. 25 (2021) 6056–6069.
[9] J.Y. Sung, S.G. Kim, D.H. Cho, J.R. Kim, H.C. Choi, SRT1720-induced activation of SIRT1 alleviates vascular smooth muscle cell senescence through PKA-dependent phosphorylation of AMPKα at Ser485, FEBS Open Bio 10 (2020) 1316–1325.
[10] J. Wang, X. Song, G. Tan, P. Sun, L. Guo, N. Zhang, J. Wang, B. Li, NAD+ improved experimental autoimmune encephalomyelitis by regulating SIRT1 to inhibit PI3K/Akt/mTOR signaling pathway, Aging (Albany NY) 13 (2021) 25931–25943.
[11] C. Pi, Y. Yang, Y. Sun, H. Wang, H. Sun, M. Ma, L. Lin, Y. Shi, Y. Li, Y. Li, X. He, Nicotinamide phosphoribosyltransferase postpones rat bone marrow mesenchymal stem cell senescence by mediating NAD(+)-Sirt1 signaling, Aging (Albany NY) 11 (2019) 3505–3522.
[12] J. Wang, L. Liu, Z. Ding, Q. Luo, Y. Ju, G. Song, Exogenous NAD(+) postpones the D-gal-induced senescence of bone marrow-derived mesenchymal stem cells via Sirt1 signaling, Antioxidants (2021) 10.
[13] D.J. Li, F. Huang, M. Ni, H. Fu, L.S. Zhang, F.M. Shen, α7 nicotinic acetylcholine receptor relieves angiotensin II-induced senescence in vascular smooth muscle cells by raising nicotinamide adenine dinucleotide-dependent SIRT1 activity, Arterioscler. Thromb. Vasc. Biol. 36 (2016) 1566–1576.
[14] J. Yoshino, J.A. Baur, S.I. Imai, NAD(+) intermediates: the biology and therapeutic potential of NMN and NR, Cell Metabol. 27 (2018) 513–528.
[15] F.J. Martínez-Morcillo, J. Cantón-Sandoval, T. Martínez-Menchón, R. Corbalán-Vélez, P. Mesa-Del-Castillo, A.B. Pérez-Oliva, D. García-Moreno, V. Mulero, Non-canonical roles of NAMPT and PARP in inflammation, Dev. Comp. Immunol. 115 (2021), 103881.
[16] A. Garten, S. Schuster, M. Penke, T. Gorski, T. de Giorgis, W. Kiess, Physiological and pathophysiological roles of NAMPT and NAD metabolism, Nat. Rev. Endocrinol. 11 (2015) 535–546.
[17] F.D. Khaidizar, Y. Bessho, Y. Nakahata, Nicotinamide phosphoribosyltransferase as a key molecule of the aging/senescence process, Int. J. Mol. Sci. (2021) 22.
[18] E. van der Veer, C. Ho, C. O'Neil, N. Barbosa, R. Scott, S.P. Cregan, J.G. Pickering, Extension of human cell lifespan by nicotinamide phosphoribosyltransferase, J. Biol. Chem. 282 (2007) 10841–10845.
[19] H. Yang, Y. Hong, Y. Lin, X. Li, [Role of nicotinamide phosphoribosyltransferase in delaying smooth muscle cell senescence and protecting abdominal aortic aneurysm], Zhonghua Wei Zhong Bing Ji Jiu Yi Xue 34 (2022) 646–650.
[20] P. Sharma, J. Xu, K. Williams, M. Easley, J.B. Elder, R. Lonser, F.F. Lang, R. Lapalombella, D. Sampath, V.K. Puduvalli, Inhibition of nicotinamide phosphoribosyltransferase (NAMPT), the rate-limiting enzyme of the nicotinamide adenine dinucleotide (NAD) salvage pathway, to target glioma heterogeneity through mitochondrial oxidative stress, Neuro Oncol. 24 (2022) 229–244.
[21] V.I. Summerhill, V.N. Sukhorukov, A.H. Eid, L.V. Nedosugova, I.A. Sobenin, A. N. Orekhov, Pathophysiological aspects of the development of abdominal aortic aneurysm with a special focus on mitochondrial dysfunction and genetic associations, Biomol. Concepts 12 (2021) 55–67.
[22] A.K. Sharma, G. Lu, A. Jester, W.F. Johnston, Y. Zhao, V.A. Hajzus, M. R. Saadatzadeh, G. Su, C.M. Bhamidipati, G.S. Mehta, et al., Experimental abdominal aortic aneurysm formation is mediated by IL-17 and attenuated by mesenchymal stem cell treatment, Circulation 126 (2012) S38–S45.
[23] S. Rani, A.E. Ryan, M.D. Griffin, T. Ritter, Mesenchymal stem cell-derived extracellular vesicles: toward cell-free therapeutic applications, Mol. Ther. 23 (2015) 812–823.
[24] S. Varderidou-Minasian, M.J. Lorenowicz, Mesenchymal stromal/stem cell-derived extracellular vesicles in tissue repair: challenges and opportunities, Theranostics 10 (2020) 5979–5997.
[25] T.Z. Nazari-Shafti, S. Neuber, A. Garcia Duran, Z. Xu, E. Beltsios, M. Seifert, V. Falk, C. Stamm, Human mesenchymal stromal cells and derived extracellular vesicles: translational strategies to increase their proangiogenic potential for the treatment of cardiovascular disease, Stem Cells Transl Med 9 (2020) 1558–1569.
[26] J.Y. Lee, J. Chung, Y. Byun, K.H. Kim, S.H. An, K. Kwon, Mesenchymal stem cell-derived small extracellular vesicles protect cardiomyocytes from doxorubicin-induced cardiomyopathy by upregulating survivin expression via the miR-199a-3p-Akt-Sp1/p53 signaling pathway, Int. J. Mol. Sci. (2021) 22.
[27] M. Kozakai, Y. Narita, A. Yamawaki-Ogata, K.L. Fujimoto, M. Mutsuga, Y. Tokuda, A. Usui, Alternative therapeutic strategy for existing aortic aneurysms using mesenchymal stem cell-derived exosomes, Expet Opin. Biol. Ther. 22 (2022) 95–104.
[28] C.G. Kim, J.K. Lee, G.J. Cho, O.S. Shin, J.A. Gim, Small RNA sequencing of small extracellular vesicles secreted by umbilical cord mesenchymal stem cells following replicative senescence, Genes Genomics 45 (2023) 347–358.
[29] R. Huang, C. Qin, J. Wang, Y. Hu, G. Zheng, G. Qiu, M. Ge, H. Tao, Q. Shu, J. Xu, Differential effects of extracellular vesicles from aging and young mesenchymal stem cells in acute lung injury, Aging (Albany NY) 11 (2019) 7996–8014.
[30] Q. Lian, Y. Zhang, X. Liang, F. Gao, H.F. Tse, Directed differentiation of human-induced pluripotent stem cells to mesenchymal stem cells, Methods Mol. Biol. 1416 (2016) 289–298.
[31] Q. Lian, Y. Zhang, J. Zhang, H.K. Zhang, X. Wu, Y. Zhang, F.F. Lam, S. Kang, J. C. Xia, W.H. Lai, et al., Functional mesenchymal stem cells derived from human induced pluripotent stem cells attenuate limb ischemia in mice, Circulation 121 (2010) 1113–1123.
[32] Y. Zhang, X. Liang, S. Liao, W. Wang, J. Wang, X. Li, Y. Ding, Y. Liang, F. Gao, M. Yang, et al., Potent paracrine effects of human induced pluripotent stem cell-derived mesenchymal stem cells attenuate doxorubicin-induced cardiomyopathy, Sci. Rep. 5 (2015), 11235.

[33] H. Zheng, X. Liang, Q. Han, Z. Shao, Y. Zhang, L. Shi, Y. Hong, W. Li, C. Mai, Q. Mo, et al., Hemin enhances the cardioprotective effects of mesenchymal stem cell-derived exosomes against infarction via amelioration of cardiomyocyte senescence, J. Nanobiotechnol. 19 (2021) 332.
[34] J. Sun, H. Shen, L. Shao, X. Teng, Y. Chen, X. Liu, Z. Yang, Z. Shen, HIF-1α overexpression in mesenchymal stem cell-derived exosomes mediates cardioprotection in myocardial infarction by enhanced angiogenesis, Stem Cell Res. Ther. 11 (2020) 373.
[35] W.X. Gao, Y.Q. Sun, J. Shi, C.L. Li, S.B. Fang, D. Wang, X.Q. Deng, W. Wen, Q.L. Fu, Effects of mesenchymal stem cells from human induced pluripotent stem cells on differentiation, maturation, and function of dendritic cells, Stem Cell Res. Ther. 8 (2017) 48.
[36] S.B. Fang, H.Y. Zhang, X.C. Meng, C. Wang, B.X. He, Y.Q. Peng, Z.B. Xu, X.L. Fan, Z. J. Wu, Z.C. Wu, et al., Small extracellular vesicles derived from human MSCs prevent allergic airway inflammation via immunomodulation on pulmonary macrophages, Cell Death Dis. 11 (2020) 409.
[37] Y.Q. Peng, Z.C. Wu, Z.B. Xu, S.B. Fang, D.H. Chen, H.Y. Zhang, X.Q. Liu, B.X. He, D. Chen, C.A. Akdis, Q.L. Fu, Mesenchymal stromal cells-derived small extracellular vesicles modulate DC function to suppress Th2 responses via IL-10 in patients with allergic rhinitis, Eur. J. Immunol. 52 (2022) 1129–1140.
[38] W. You, Y. Hong, H. He, X. Huang, W. Tao, X. Liang, Y. Zhang, X. Li, TGF-beta mediates aortic smooth muscle cell senescence in Marfan syndrome, Aging (Albany NY) 11 (2019) 3574–3584.
[39] W. You, Y. Hong, H. He, X. Huang, W. Tao, X. Liang, Y. Zhang, X. Li, TGF-β mediates aortic smooth muscle cell senescence in Marfan syndrome, Aging (Albany NY) 11 (2019) 3574–3584.
[40] T. Stuart, A. Butler, P. Hoffman, C. Hafemeister, E. Papalexi, W.M. Mauck 3rd, Y. Hao, M. Stoeckius, P. Smibert, R. Satija, Comprehensive integration of single-cell data, Cell 177 (2019) 1888–1902 e1821.
[41] A. Butler, P. Hoffman, P. Smibert, E. Papalexi, R. Satija, Integrating single-cell transcriptomic data across different conditions, technologies, and species, Nat. Biotechnol. 36 (2018) 411–420.
[42] Y. Hao, S. Hao, E. Andersen-Nissen, W.M. Mauck 3rd, S. Zheng, A. Butler, M.J. Lee, A.J. Wilk, C. Darby, M. Zager, et al., Integrated analysis of multimodal single-cell data, Cell 184 (2021) 3573–3587.e3529.
[43] T. Stuart, A. Butler, P. Hoffman, C. Hafemeister, E. Papalexi, W.M. Mauck 3rd, Y. Hao, M. Stoeckius, P. Smibert, R. Satija, Comprehensive integration of single-cell data, Cell 177 (2019) 1888–1902.e1821.
[44] C. Yap, A. Mieremet, C.J.M. de Vries, D. Micha, V. de Waard, Six shades of vascular smooth muscle cells illuminated by KLF4 (Kruppel-Like factor 4), Arterioscler. Thromb. Vasc. Biol. 41 (2021) 2693–2707.
[45] H.Y. Tang, A.Q. Chen, H. Zhang, X.F. Gao, X.Q. Kong, J.J. Zhang, Vascular smooth muscle cells phenotypic switching in cardiovascular diseases, Cells (2022) 11.
[46] A. Chakraborty, Y. Li, C. Zhang, Y. Li, K.R. Rebello, S. Li, S. Xu, H.G. Vasquez, L. Zhang, W. Luo, et al., Epigenetic induction of smooth muscle cell phenotypic alterations in aortic aneurysms and dissections, Circulation 148 (2023) 959–977.
[47] G. Cao, X. Xuan, J. Hu, R. Zhang, H. Jin, H. Dong, How vascular smooth muscle cell phenotype switching contributes to vascular disease, Cell Commun. Signal. 20 (2022) 180.
[48] Q. Wang, Y. Ding, P. Song, H. Zhu, I. Okon, Y.N. Ding, H.Z. Chen, D.P. Liu, M. H. Zou, Tryptophan-derived 3-hydroxyanthranilic acid contributes to angiotensin II-induced abdominal aortic aneurysm formation in mice in vivo, Circulation 136 (2017) 2271–2283.
[49] L.Y. Sun, Y.Y. Lyu, H.Y. Zhang, Z. Shen, G.Q. Lin, N. Geng, Y.L. Wang, L. Huang, Z. H. Feng, X. Guo, et al., Nuclear receptor NR1D1 regulates abdominal aortic aneurysm development by targeting the mitochondrial tricarboxylic acid cycle enzyme aconitase-2, Circulation 146 (2022) 1591–1609.
[50] C.L. Liu, X. Liu, Y. Zhang, J. Liu, C. Yang, S. Luo, T. Liu, Y. Wang, J.S. Lindholt, A. Diederichsen, et al., Eosinophils protect mice from angiotensin-II perfusion-induced abdominal aortic aneurysm, Circ. Res. 128 (2021) 188–202.
[51] A. Daugherty, L.A. Cassis, Mouse models of abdominal aortic aneurysms, Arterioscler. Thromb. Vasc. Biol. 24 (2004) 429–434.
[52] A. Daugherty, M.W. Manning, L.A. Cassis, Angiotensin II promotes atherosclerotic lesions and aneurysms in apolipoprotein E-deficient mice, J. Clin. Invest. 105 (2000) 1605–1612.
[53] T. Horimatsu, A.L. Blomkalns, M. Ogbi, M. Moses, D. Kim, S. Patel, N. Gilreath, L. Reid, T.W. Benson, J. Pye, et al., Niacin protects against abdominal aortic aneurysm formation via GPR109A independent mechanisms: role of NAD+/nicotinamide, Cardiovasc. Res. 116 (2020) 2226–2238.
[54] S. Wang, Z. Xing, P.S. Vosler, H. Yin, W. Li, F. Zhang, A.P. Signore, R.A. Stetler, Y. Gao, J. Chen, Cellular NAD replenishment confers marked neuroprotection against ischemic cell death: role of enhanced DNA repair, Stroke 39 (2008) 2587–2595.
[55] A. Watson, Z. Nong, H. Yin, C. O'Neil, S. Fox, B. Balint, L. Guo, O. Leo, M.W.A. Chu, R. Gros, J.G. Pickering, Nicotinamide phosphoribosyltransferase in smooth muscle cells maintains genome integrity, resists aortic medial degeneration, and is suppressed in human thoracic aortic aneurysm disease, Circ. Res. 120 (2017) 1889–1902.
[56] W. Xu, Y. Chao, M. Liang, K. Huang, C. Wang, CTRP13 mitigates abdominal aortic aneurysm formation via NAMPT1, Mol. Ther. 29 (2021) 324–337.
[57] Y. Li, Y. Zhang, B. Dorweiler, D. Cui, T. Wang, C.W. Woo, C.S. Brunkan, C. Wolberger, S. Imai, I. Tabas, Extracellular Nampt promotes macrophage survival via a nonenzymatic interleukin-6/STAT3 signaling mechanism, J. Biol. Chem. 283 (2008) 34833–34843.
[58] T. Kitani, S. Okuno, H. Fujisawa, Growth phase-dependent changes in the subcellular localization of pre-B-cell colony-enhancing factor, FEBS Lett. 544 (2003) 74–78.
[59] M. Dalamaga, G.S. Christodoulatos, C.S. Mantzoros, The role of extracellular and intracellular Nicotinamide phosphoribosyl-transferase in cancer: diagnostic and therapeutic perspectives and challenges, Metabolism 82 (2018) 72–87.
[60] M. Hasmann, I. Schemainda, FK866, a highly specific noncompetitive inhibitor of nicotinamide phosphoribosyltransferase, represents a novel mechanism for induction of tumor cell apoptosis, Cancer Res. 63 (2003) 7436–7442.
[61] H. Yan, H.F. Zhou, A. Akk, Y. Hu, L.E. Springer, T.L. Ennis, C.T.N. Pham, Neutrophil proteases promote experimental abdominal aortic aneurysm via extracellular trap release and plasmacytoid dendritic cell activation, Arterioscler. Thromb. Vasc. Biol. 36 (2016) 1660–1669.
[62] A. Golchin, T.Z. Farahany, Biological products: cellular therapy and FDA approved products, Stem Cell Rev Rep 15 (2019) 166–175.
[63] K.S. Park, E. Bandeira, G.V. Shelke, C. Lasser, J. Lotvall, Enhancement of therapeutic potential of mesenchymal stem cell-derived extracellular vesicles, Stem Cell Res. Ther. 10 (2019) 288.
[64] X. Zhu, M. Badawi, S. Pomeroy, D.S. Sutaria, Z. Xie, A. Baek, J. Jiang, O. A. Elgamal, X. Mo, K. Perle, et al., Comprehensive toxicity and immunogenicity studies reveal minimal effects in mice following sustained dosing of extracellular vesicles derived from HEK293T cells, J. Extracell. Vesicles 6 (2017), 1324730.
[65] B. Lukomska, L. Stanaszek, E. Zuba-Surma, P. Legosz, S. Sarzynska, K. Drela, Challenges and controversies in human mesenchymal stem cell therapy, 2019, Stem Cell. Int. (2019), 9628536.
[66] L. Sun, R. Xu, X. Sun, Y. Duan, Y. Han, Y. Zhao, H. Qian, W. Zhu, W. Xu, Safety evaluation of exosomes derived from human umbilical cord mesenchymal stromal cell, Cytotherapy 18 (2016) 413–422.
[67] M. Lu, L. Peng, X. Ming, X. Wang, A. Cui, Y. Li, X. Wang, D. Meng, N. Sun, M. Xiang, S. Chen, Enhanced wound healing promotion by immune response-free monkey autologous iPSCs and exosomes vs. their allogeneic counterparts, EBioMedicine 42 (2019) 443–457.
[68] G. Wu, Q. Su, J. Li, C. Xue, J. Zhu, Q. Cai, J. Huang, S. Ji, B. Cheng, H. Ge, NAMPT encapsulated by extracellular vesicles from young adipose-derived mesenchymal stem cells treated tendinopathy in a "One-Stone-Two-Birds" manner, J. Nanobiotechnol. 21 (2023) 7.
[69] M. Yoshida, A. Satoh, J.B. Lin, K.F. Mills, Y. Sasaki, N. Rensing, M. Wong, R. S. Apte, S.I. Imai, Extracellular vesicle-contained eNAMPT delays aging and extends lifespan in mice, Cell Metabol. 30 (2019) 329–342 e325.
[70] M.C. Chong, A. Silva, P.F. James, S.S.X. Wu, J. Howitt, Exercise increases the release of NAMPT in extracellular vesicles and alters NAD(+) activity in recipient cells, Aging Cell 21 (2022), e13647.
[71] P. Neupane, S. Bhuju, N. Thapa, H.K. Bhattarai, ATP synthase: structure, function and inhibition, Biomol. Concepts 10 (2019) 1–10.
[72] K. Yuan, W. Liang, J. Zhang, A comprehensive analysis of differentially expressed genes and pathways in abdominal aortic aneurysm, Mol. Med. Rep. 12 (2015) 2707–2714.
[73] E. Biros, G. Gabel, C.S. Moran, C. Schreurs, J.H. Lindeman, P.J. Walker, M. Nataatmadja, M. West, L.M. Holdt, I. Hinterseher, et al., Differential gene expression in human abdominal aortic aneurysm and aortic occlusive disease, Oncotarget 6 (2015) 12984–12996.
[74] F.M. Davis, L.C. Tsoi, F. Ma, R. Wasikowski, B.B. Moore, S.L. Kunkel, J. E. Gudjonsson, K.A. Gallagher, Single-cell transcriptomics reveals dynamic role of smooth muscle cells and enrichment of immune cell subsets in human abdominal aortic aneurysms, Ann. Surg. 276 (2022) 511–521.
[75] P. Gao, H. Zhang, Q. Zhang, X. Fang, H. Wu, M. Wang, Z. Lu, X. Wei, G. Yang, Z. Yan, et al., Caloric restriction exacerbates angiotensin II-induced abdominal aortic aneurysm in the absence of p53, Hypertension 73 (2019) 547–560.